e-ISSN : 3089-7783
p-ISSN : xxxx-xxxx

JAMAT

VOLUME 2 (NO 1) JUNE 2025

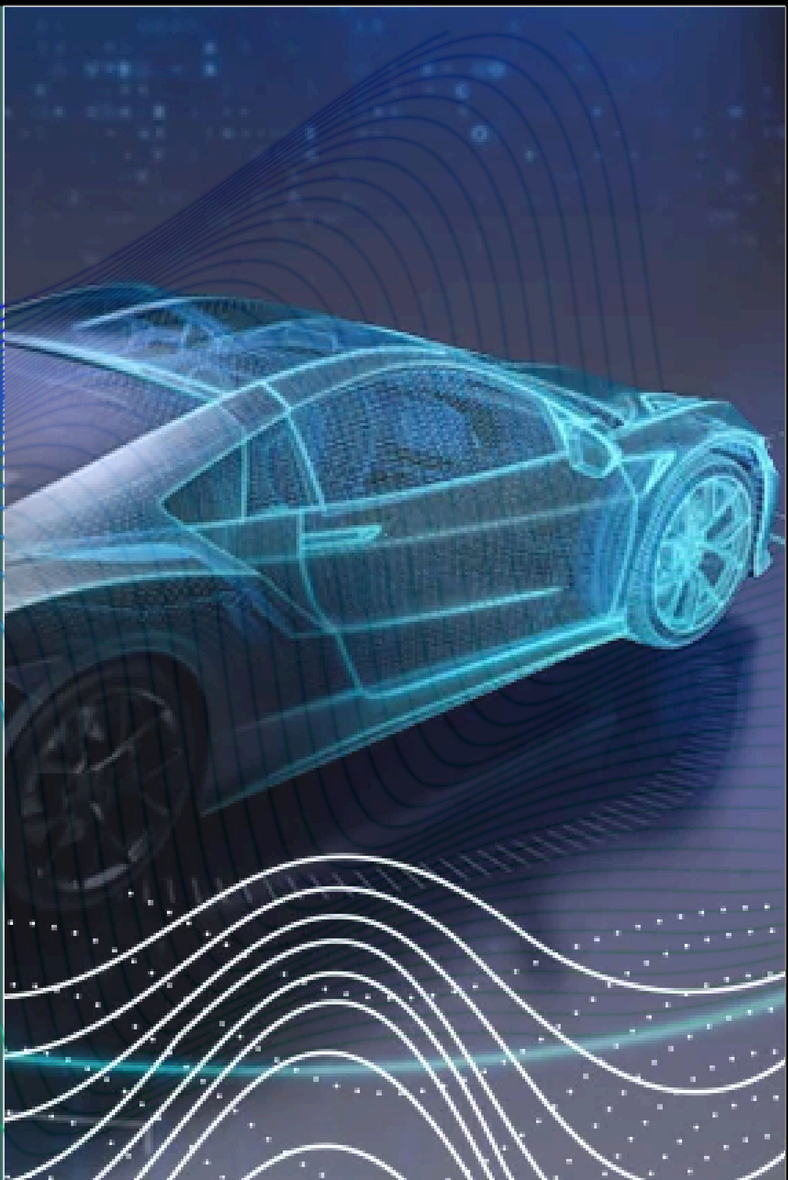

Journal of Automotive and Mechanical Applied Technology

Published by
Department of Mechanical and
Automotive Engineering
Faculty of Vocational
Universitas Negeri Yogyakarta

Journal of
Automotive and Mechanical Applied Technology
Volume 2, Nomor 1, June 2025

JAMAT EDITORS

EDITOR-IN-CHEF
Agus Widyianto
Department of Mechanical and Automotive Engineering, Faculty of Vocational, UNY
Kampus Kulon Progo, Yogyakarta

ASSOCIATE (MAIN HANDLING) EDITORS
Muhammad Imawan Badranaya
Department of Mechanical and Automotive Engineering, Faculty of Vocational, UNY
Kampus Kulon Progo, Yogyakarta

Aan Yudianto
Department of Mechanical and Automotive Engineering, Faculty of Vocational, UNY
Kampus Kulon Progo, Yogyakarta

Yoga Guntur Sampurno
Department of Mechanical and Automotive Engineering, Faculty of Vocational, UNY
Kampus Kulon Progo, Yogyakarta

Rita Fransina Maruanaya
Fakultät Erziehungswissenschaften, Technische Universitat Dresden, Germany

Journal of
Automotive and Mechanical Applied Technology
Volume 2, Nomor 1, June 2025

Table of Contents

JOURNAL OF AUTOMOTIVE AND MECHANICAL APPLIED TECHNOLOGY

Vol. 2 No. 1, 2025, pp. 66-75 https://journal.uny.ac.id/publications/jamat https://doi.org/10.21831/jamat.v2i1.1277

Development of a Real-Time Vibration Monitoring System for Drum Tester Machines Using ADXL345 Sensor and ESP32 Microcontroller

Herdiansyah Noorrizky Anggana[1], Moch Solikin[1*]

[1]Department of Mechanical and Automotive Engineering, Faculty of Vocational, Universitas Negeri Yogyakarta, Kulonprogo, Yogyakarta 55652, Indonesia

*Corresponding author: moch_solikin@uny.ac.id

ARTICLE INFO

Article history:

Received 23.01.2025

Revised 20.02.2025

Accepted 10.03.2025

Keywords:

Vibration Monitoring; ADXL345 Sensor; ESP32 Microcontroller; Real-Time System

ABSTRACT

This study focuses on developing a vibration level monitoring system for a drum tester machine, utilizing the ADXL345 sensor in conjunction with the ESP32 microcontroller and a web-based monitoring platform. The system was implemented at PT Astra Daihatsu Motor's Sunter Assembly Plant (SAP) located in Jakarta, Indonesia, for large-scale industrial use. The design aimed to boost precision in vibration monitoring and elevate workforce productivity. The sensor collects data, which is then sent to a MySQL database and shown in real-time on an LCD and through a Grafana-based web interface. Functional tests verified that all components performed as specified. The ESP32 microcontroller provided reliable Wi-Fi connectivity, and the ADXL345 sensor showed impressive accuracy in detecting vibration changes in both static and dynamic situations. Performance tests conducted over eight hours, with data collected at one-minute intervals, demonstrated consistent readings across all axes (X, Y, Z), highlighting the system's reliability. The implementation of this system resulted in enhanced efficiency in machine monitoring. The inspection interval has been extended from two weeks to one month, which has reduced the workforce requirements from two workers to one. Moreover, the time required for inspection was reduced from 20 minutes to only one minute. To summarize, this vibration monitoring system enhances the accuracy of real-time data, improves workforce efficiency, and ensures reliable monitoring of machine conditions. This offers a creative approach for industrial uses, enhancing operational efficiency and ensuring workplace safety.

1. Introduction

PT Astra Daihatsu Motor (ADM) is the sole brand holder agent (ATPM) for Daihatsu vehicles in Indonesia, authorized for the importation, assembly, and production of Daihatsu and Toyota-branded vehicles and related components [1]. Since its establishment in 1978, ADM has operated through several manufacturing facilities, one of which is the Sunter Assembly Plant (SAP) located in Jakarta. SAP has an annual production capacity of 330,000 units, with an average production time of 81 seconds per unit. In 2023, there was a significant increase in vehicle sales, particularly for the Gran Max model, which reached 32,000 units, accounting for 21.8% of total distribution between January and June.

As production volume continues to rise, efficiency and quality have become crucial factors in maintaining the company's competitiveness. Defect-free production is crucial for ensuring customer satisfaction and fostering long-term sales growth [2]. Therefore, the Quality Control (QC) division plays a vital role in ensuring that every unit produced meets the required quality standards before being distributed to customers [3]. One of the primary processes in Quality Control Inspection is the use of a drum tester [4], a testing device designed to verify the performance of vehicle indicators such as wipers, high beams, and dashboard indicators by running the vehicle at a speed of 60 km/h on a rotating drum. However, quality inspections using the drum tester face significant challenges, particularly in terms of maintenance [5, 6].

However, this process faces a major challenge, frequent maintenance issues with the pillow block bearings of the drum tester, particularly due to bearing wear and inadequate lubrication. These issues lead to excessive vibrations, causing operational inefficiencies, safety risks, and increased downtime [7, 8]. Currently, inspections are conducted manually every two weeks, taking about 20 minutes per session and requiring two personnel, which is both time-consuming and resource-intensive.

To overcome these limitations, this study proposes the development of a real-time IoT-based vibration monitoring system utilizing the ADXL345 accelerometer sensor and the ESP32 microcontroller [9, 10]. The system aims to automatically detect and report abnormal vibrations, enabling predictive maintenance and minimizing unscheduled downtimes. This is a direct response to the identified problems, including manual inspections, late fault detection, and inefficient workforce deployment.

Furthermore, the integration of the system with digital platforms such as MySQL databases and Grafana dashboards enables centralized and remote monitoring, significantly improving accessibility and decision-making. Looking forward, this system is also scalable and compatible with Artificial Intelligence (AI) and Big Data technologies, which can be used to analyze historical vibration patterns for predictive analytics and machine learning models. These enhancements will support the adoption of smart maintenance strategies and align with Industry 4.0 goals by transitioning from reactive to proactive maintenance approaches [11].

2. Methodology

A real-time vibration monitoring system is the main topic of this study. It is designed and implemented utilizing the ADXL345 accelerometer, ESP32 microcontroller, MySQL database, and Grafana visualization platform. The research consisted of four main phases: analysis of demands, system implementation, manufacturing (including PCB and enclosure design), and testing. There is also a detailed outline of the testing processes and system architecture.

2.1 Need Analysis

At this stage, an identification process was carried out to determine the necessary system for monitoring machine vibrations, particularly on the pillow block bearing of the drum tester at PT Astra Daihatsu Motor. The primary requirements include vibration measurement accuracy, data storage in MySQL [12], and data visualization through Grafana [13]. The ADXL345 sensor was selected due to its capability to measure vibrations along three axes [14, 15]. At the same time, the ESP32 microcontroller was used to connect the system to a Wi-Fi network. The hardware and its specifications are presented in Table 1, while the software and its specifications are shown in Table 2.

Table 1. Hardware used in the system

No	Component	Specification
1	Battery 16850	3.7 V, 2.5 – 3.5 A
2	On/Off Switch	2A
3	ESP32 microcontroller	Dual-core, Wi-Fi, Bluetooth, 2.4 GHz, 240 MHz, 520 KB SRAM, 4 MB Flash, 3.3 V.
4	Adxl345 accelerometer sensor	3-Axis (X, Y, Z), ±2g/±4g/±8g/±16g range, I2C/SPI interface, 2 – 3.6 V
5	Stepdown	Input 4.5-28 V, Output 0.8-20 V, 3A max
6	LCD I2C	16x2 character, I2C interface, 5V
7	AWG24 cable	300V Max

No	Component	Specification
8	Box	150mmx100mmx65mm
9	Plate	20mmx15mmx10mm

Table 2. Software used in the system

Software	Usability
Arduino IDE	Used to program the ESP32 microcontroller
Notepad++ PhP	Used to program data from the microcontroller into the database
MySQL	Used as a storage database
Grafana	Used to visualize data.

The first step in resolving the ongoing maintenance problems with the drum tester was to survey PT Astra Daihatsu Motor for signs of wear and vibration-related bearing failures in the pillow block. In order to resolve these concerns, essential system needs were determined, which comprise: Reliable detection of vibrations along the X, Y, and Z axes. The transmission and display of data in real-time. The ability to connect to Grafana and other web-based monitoring tools. Recording vibration data for future reference.

Due to its compact size, I²C/SPI interface, and sensitivity across a wide range of accelerations (±2g to ±16g), the ADXL345 sensor was selected. The ESP32 microcontroller was chosen due to its interoperability with Internet of Things applications, built-in Wi-Fi, and dual-core computing capabilities.

2.2 Implementation

The complete system architecture consists of the following subsystems. The mechanical design was developed to position the ADXL345 sensor on the drum tester machine. The electronic circuit design involved connecting the sensor to the ESP32 microcontroller using the I2C communication protocol. The software was developed using Arduino IDE to read sensor data, transmit it to a MySQL database, and display the results on Grafana. The Arduino code enables the ESP32 to connect the ADXL345 sensor to Wi-Fi and transmit data to the MySQL database. Grafana is utilized to visualize vibration data in a graphical form.

2.3 Manufacturing

The PCB was designed using Wokwi simulation software to ensure proper routing and minimal signal interference. After fabrication, continuity tests, voltage validation, and I2C communication checks were performed using a multimeter and oscilloscope to verify performance under operating conditions. The PCB was designed using Wokwi software, and the components were carefully soldered. All circuits were tested to ensure proper connections. The device enclosure was designed using AutoCAD and SolidWorks to house the electronic components and sensors. The enclosure was then cut and assembled according to the design specifications.

2.4 Testing

System testing involved three stages: electrical testing, functional testing, and performance testing under operational conditions. All vibration data was analyzed based on ISO 10816-3: Mechanical vibration – Evaluation of machine vibration by measurements on non-rotating parts. This standard provides classification criteria for vibration severity in industrial machines. Data collected from the ADXL345 was converted to velocity (mm/s) and compared against the following standard zones: Zona A (Green), Zona B (Yellow), Zona C (Orange), and Zona D (Red).

The testing was conducted at PT. Astra Daihatsu Motor ensures that each component of the system functions properly. Hardware testing involved verifying the voltage levels on the ESP32 and ADXL345 sensor. In contrast, software testing ensured that sensor data was successfully transmitted to the MySQL database and displayed on Grafana. The testing was conducted by connecting the device to a power source and activating the MySQL database along with the Grafana web interface. The machine was subjected to vibrations, and the resulting vibration data was observed to ensure the accuracy of the sensor readings. The ISO 10816-3 [9] standard was used to measure machine vibration levels. The acquired data was categorized into different vibration severity levels: green (normal), yellow (alert), orange (critical), and red (dangerous), as illustrated in Fig. 1.

<table>
<tr><th colspan="2">Velocity Severety</th><th colspan="4">Velocity Range Limits and Machine Classes
ISO Standard 10816</th></tr>
<tr><th rowspan="2">Mm/s RMS</th><th rowspan="2">In/s Peak</th><th rowspan="2">Small Machines Class I</th><th rowspan="2">Medium Machines Class II</th><th colspan="2">Large Machines</th></tr>
<tr><th>Rigid Supports Class III</th><th>Less Rigid Supports Class IV</th></tr>
<tr><td>0.25</td><td>0.02</td><td rowspan="3">Good</td><td rowspan="4">Good</td><td rowspan="5">Good</td><td rowspan="6">Good</td></tr>
<tr><td>0.45</td><td>0.03</td></tr>
<tr><td>0.71</td><td>0.04</td></tr>
<tr><td>1.12</td><td>0.06</td><td rowspan="2">Statisfactory</td></tr>
<tr><td>1.83</td><td>0.10</td><td rowspan="2">Statisfactory</td></tr>
<tr><td>2.80</td><td>0.16</td><td rowspan="2">Unstatisfactory (Alert)</td><td rowspan="2">Statisfactory</td></tr>
<tr><td>4.50</td><td>0.25</td><td rowspan="2">Unstatisfactory (Alert)</td><td rowspan="2">Statisfactory</td></tr>
<tr><td>7.10</td><td>0.40</td><td rowspan="5">Unacceptable (Danger)</td><td rowspan="2">Unstatisfactory (Alert)</td></tr>
<tr><td>11.2</td><td>0.62</td><td rowspan="4">Unacceptable (Danger)</td><td rowspan="2">Unstatisfactory (Alert)</td></tr>
<tr><td>18.0</td><td>1.00</td><td rowspan="3">Unacceptable (Danger)</td></tr>
<tr><td>28.0</td><td>1.56</td><td rowspan="2">Unacceptable (Danger)</td></tr>
<tr><td>40.0</td><td>2.51</td></tr>
</table>

Figure 1. Level of vibration (ISO 10816-3)

3. Result and Discussion

3.1 Design and manufacture

In this study, a vibration monitoring system for the drum tester machine's pillow block bearing has been successfully developed. The system utilizes an ADXL345 sensor connected to a NodeMCU ESP32 microcontroller to monitor vibration levels in real time. The acquired data is transmitted and stored in a MySQL database and can be accessed through a monitoring interface using Grafana [16]. The development process began with a needs assessment and problem analysis. Field observations revealed that workers had to physically inspect the machine in the lower area, posing a risk of workplace accidents. To address this issue, a monitoring system capable of storing historical data online was implemented. The system design consists of both hardware and software components. The hardware includes a mechanical design created using AutoCAD and an electrical design developed using Fritzing. The software involves programming the microcontroller with Arduino IDE, as well as data processing and monitoring visualization through Grafana.

3.2 Product testing

The functional testing phase was conducted to ensure that each system component operates according to the predefined specifications. Key components, including the NodeMCU ESP32, LCD I2C 16x2, ADXL345 sensor, and ON/OFF button, were individually tested to assess their performance and compliance with the designed technical characteristics. This testing process involved verifying electrical performance, data communication, and the primary functionality of each module. Additionally, the integration of all components was examined to ensure the system operates synergistically without errors or data processing issues.

During the ESP32 microcontroller testing, an evaluation was performed to assess the stability of the power supply and network connectivity, which are critical aspects of system reliability. The test results indicated that the ESP32 functioned effectively within its specifications, maintaining stable operating voltage and uninterrupted Wi-Fi connectivity. The success of this testing confirms that the microcontroller module is a reliable central control unit for the system. The electrical verification results for the ESP32 are presented in Table 3.

Table 3. ESP32 verification result

Testing	Input (Volt)	Output (Volt)
Pin GND	5V	5.02
Pin3.3V	5V	3.28
D212 (SCL)	-	3.26
D22 (SDA	-	3.26

The ADXL345 sensor was tested to evaluate its accuracy in detecting changes in vibration acceleration. The tests were performed under both static and dynamic conditions to observe the sensor's response to applied vibrations. The results indicated that the sensor could accurately detect acceleration variations, both in a no-vibration state and when subjected to external shocks. The generated data consistently aligned with theoretical predictions, confirming that the ADXL345 sensor functions as expected. The electrical verification results for the ADXL345 sensor are presented in Table 4.

Table 4. ADLX345 verification result

Testing	Input (mm/s)	Output (mm/s)	%Error
X Acceleration	9.81	9.78	0.31
Y Acceleration	-9.81	-9.75	0.61
Z Acceleration	0	0.01	0.10

To ensure that the device is calibrated correctly and capable of displaying accurate values according to its function, functional testing was conducted by collecting data under two conditions. The first condition involved recording data for five minutes while the sensor remained stationary (Fig. 2). In the second test, data were collected for five minutes while the sensor was in motion [17]. Fig. 3 presents the results of the functional testing. Based on the data, it can be determined that the sensor operates as expected, as indicated by the variations in the recorded values when the sensor was in motion.

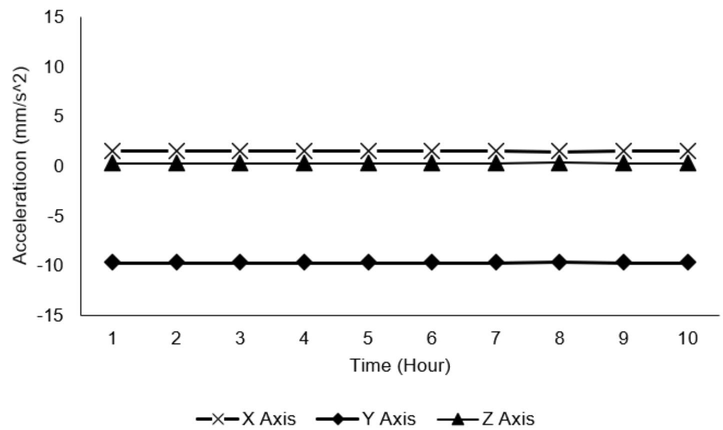

Figure 2. Sensor data in a stationary condition

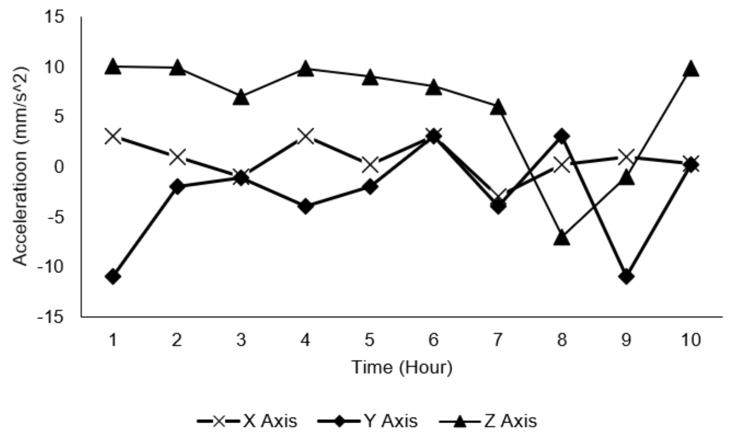

Figure 3. Sensor data in motion condition

In addition to individual component testing, an evaluation of the system's integration with the web-based monitoring platform was conducted. This test aimed to ensure that the data displayed on the LCD screen matched the information shown on the web-based monitoring interface. The results confirmed that there were no discrepancies between the data read by the hardware and the data transmitted to the monitoring system. This indicates that the data communication process between the device and the server functions reliably for long-term operation.

In addition to functional testing, performance testing was conducted to evaluate the system's capabilities under real operational conditions. The system was implemented on a drum tester machine at PT Astra Daihatsu Motor to evaluate its effectiveness in monitoring vibration levels on the pillow block bearing. The testing process covered hardware components, software functionality, LCD monitoring display, and the web-based monitoring platform. Data was collected periodically over 8 hours, with recordings taken at 1-minute intervals. The collected values were averaged hourly, resulting in a total of 8 hourly readings for further analysis.

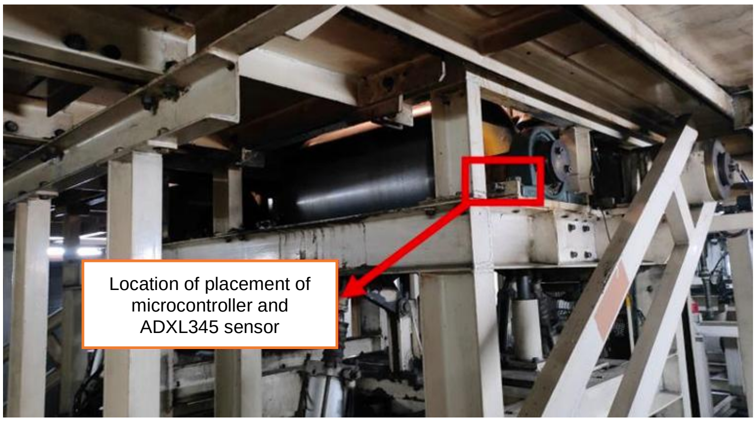

Figure 4. Installation location of the system

In this performance test, the sensor was placed on the test object (Fig. 4) and allowed to operate throughout the testing period to ensure the system's reliability in consistently reading and transmitting data. The test results showed that the data obtained from various measurement axes (X, Y, and Z) exhibited a stable trend without significant fluctuations that could indicate measurement inaccuracies (Fig. 5). This confirms that the system functions as initially designed and is capable of providing valid information regarding the machine's vibration conditions.

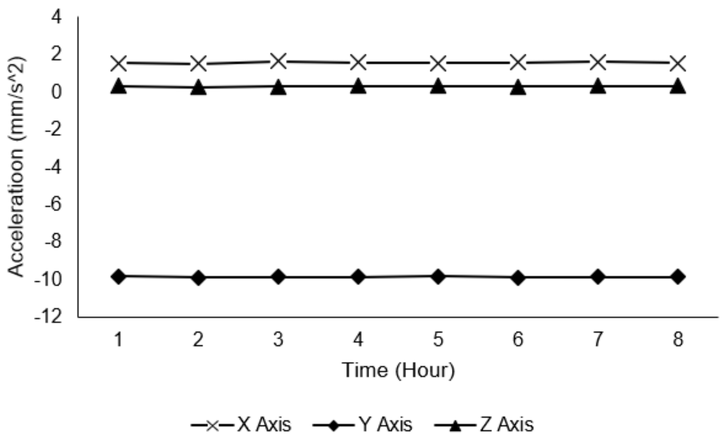

Figure 5. Measurement data result in the working condition

As a final step, verification was conducted on the displayed readings on both the LCD and the web-based monitoring system. Based on data analysis, no discrepancies were found between the data displayed on the LCD, the data stored in the MySQL database, and the data presented through the Grafana application. The dashboard display is shown in Fig. 6. This data consistency confirms that the system, both in terms of hardware and software, has operated optimally according to the specified requirements. Therefore, the developed monitoring system has been proven ready for industrial use, supporting real-time and accurate machine condition monitoring [18].

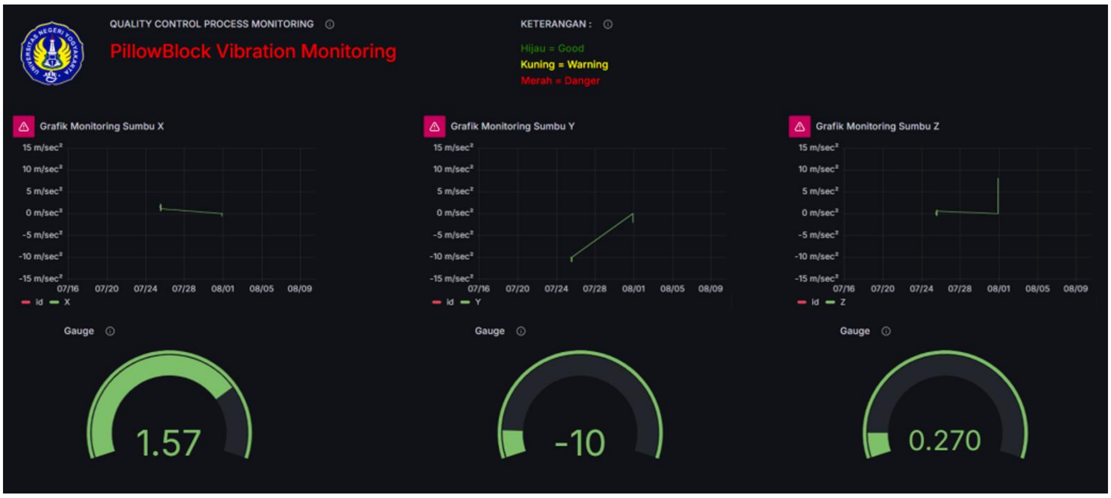

Figure 6. Measurement data results in working conditions on the dashboard interface

The implementation of this monitoring system has significantly improved workforce efficiency [19]. Prior to the system's deployment, pillow block inspections were conducted every two weeks. With the new system in place, inspections are now required only once a month, reducing the workforce needed from two workers to just one. Additionally, the inspection time has been drastically reduced from 20 minutes to just 1 minute, as workers can now check the data via a monitor without needing to go to the machine location. The improvement in system efficiency is presented in Table 5.

Table 5. Efficiency of the system usage

No	Item	Before			After		
		Period	Workforce	Inspection time	Period	Workforce	Inspection time
1	Pillow block	2 Week	2	20 Min	1 Month	1	1 Min

2	Pillow block	2 Week	2	20 Min	1 Month	1	1 Min
3	Pillow block	2 Week	2	20 Min	1 Month	1	1 Min
4	Pillow block	2 Week	2	20 Min	1 Month	1	1 Min

Thus, this system not only enhances workplace safety but also improves workforce efficiency through machine vibration monitoring.

3.3 Sensor Limitations and Noise Sources

There are several practical limitations to using the ADXL345 sensor in industrial settings, despite its reliability in detecting three-axis vibrations. Ambient noise, which can originate from nearby manufacturing or structural vibrations transmitted through the floor, is a significant concern. Vibrations from the surrounding environment can potentially degrade the sensor's performance in industrial environments when physical separation is inadequate. Electromagnetic interference (EMI) is another factor that affects measurement precision [20]. Because it uses Wi-Fi for communication, the ESP32 microcontroller is susceptible to occasional signal interference from adjacent radio-frequency (RF) sources such as routers, industrial transmitters, or wireless equipment. Nevertheless, it was noted during the system trials that EMI had a negligible effect on data transmission and integrity.

Thermal drift can also affect the sensor, particularly in hot environments or when exposed to constant heat from nearby machinery. The sensor's baseline readings can be subtly affected by long-term temperature swings, which could lead to less consistent measurements. This is why it's crucial to calibrate your device often to keep its accuracy over time. Additionally, applications that require the detection of micro-vibrations or extremely accurate diagnostics may not be well-suited to the ADXL345 sensor due to its 10-bit digital output resolution. The resolution is sufficient for most monitoring tasks, including detecting unusual vibration patterns in large mechanical components. However, it may miss more subtle changes that more sensitive sensors can detect.

The system design included multiple strategies to address and alleviate these constraints. Brackets designed to attenuate vibrations helped attach the sensor in an area where mechanical noise was minimal. To reduce transient noise and improve data clarity, the microcontroller's code also included signal smoothing techniques, such as averaging and filtering algorithms. In conclusion, the system is designed to allow for periodic calibration, ensuring that the sensor continues to provide accurate readings over time, regardless of changes in the surrounding environment.

4. Conclusion

This research successfully designed and implemented a vibration level monitoring system for drum tester machines using the ADXL345 sensor integrated with the ESP32 microcontroller and a web-based monitoring system. Based on the functional tests conducted, each system component operates efficiently by the specified requirements. The ESP32 microcontroller functions optimally with stable Wi-Fi connectivity, the ADXL345 sensor demonstrates high accuracy in measuring vibration acceleration, and the web-based monitoring system displays real-time data that is consistent with the readings shown on the LCD. Furthermore, the performance evaluation results indicate that the system can continuously monitor vibrations on the pillow block bearing for eight hours, with data recorded at one-minute intervals. The measurement results confirm the system's high reliability in detecting changes in machine vibration. Data presented in tables and graphs shows consistency between sensor readings and data stored in the MySQL database, with no significant discrepancies between the LCD readings and the web-based monitoring system.

The implementation of this monitoring system also enhances workforce efficiency. Previously, pillow block inspections were conducted biweekly; now, they are performed monthly, reducing the required workforce from two workers to one. Additionally, the inspection time has decreased significantly from 20 minutes to just one minute, as workers can now view the data on the monitor instead of physically inspecting the machine. This improvement in efficiency demonstrates that the developed system not only enhances workplace safety but also optimizes real-time monitoring of machine conditions. Thus, the vibration monitoring system, based on the ADXL345 sensor and ESP32 microcontroller, has proven effective in improving monitoring accuracy, workforce efficiency, and reliability in detecting changes in machine condition. The implementation of this system is expected to provide an innovative solution in the manufacturing industry, enhancing operational efficiency and machine safety.

Future research can enhance the current system by integrating machine learning (ML) algorithms to analyze vibration trends over time and predict potential failures before they occur. The inclusion of anomaly detection, pattern recognition, and adaptive thresholding through ML models can significantly improve predictive maintenance capabilities. Furthermore, expanding sensor types (e.g., higher-resolution accelerometers or multi-sensor arrays) and improving environmental shielding will enhance system robustness and diagnostic accuracy.

Conflict of interest

The authors declare that they have no conflict of interest.

References

[1] D. Banerjee, "Robust Car Damage Classification using CNN and KNN Algorithms," 2024: IEEE, pp. 1160-1165, doi: 10.1109/ICoICI62503.2024.10696430.

[2] J. Saragih, A. Tarigan, I. Pratama, J. Wardati, and E. F. Silalahi, "The impact of total quality management, supply chain management practices and operations capability on firm performance," *Polish Journal of Management Studies,* vol. 21, no. 2, pp. 384-397, 2020, doi: 10.17512/pjms.2020.21.2.27.

[3] M. Alhih, A. Tambi, and Y. Yusof, "Total quality management and business excellence," *International Journal of Academic Research in Business and Social Sciences,* vol. 10, no. 12, pp. 621-630, 2020.

[4] J. Ott, M. M. Marcus, T. Henderson, H. Wilson-Jene, L. Lee, and J. Pearlman, "Development and calibration of drum-based rolling resistance testing machine for manual wheelchair components," *Technology and Disability,* vol. 33, no. 2, pp. 123-136, 2021, doi: 10.3233/TAD-200285.

[5] C. Peppin, "Rotary Drum Maintenance: Follow these nine recommendations to establish a strong program for preventive maintenance of rotary drums in drying, cooling and other treatments of bulk solids," *Chemical Engineering,* vol. 130, no. 9, 2023.

[6] J. B. Camelotes *et al.*, "Application of quality control tools in analyzing defects in a drum container manufacturing industry," *Sci. Int.(Lahore),* vol. 36, no. 2, pp. 59-64, 2024.

[7] T. B. Linhares, A. da Silva Scari, and C. B. S. Vimieiro, "Causes of failures in vibrating screens: a literature review," *Minerals Engineering,* vol. 218, p. 109027, 2024, doi: https://doi.org/10.1016/j.mineng.2024.109027.

[8] I. U. Hassan, K. Panduru, and J. Walsh, "An in-depth study of vibration sensors for condition monitoring," *Sensors,* vol. 24, no. 3, p. 740, 2024, doi: https://doi.org/10.3390/s24030740.

[9] S. U. Rehman, M. Usman, M. H. Y. Toor, and Q. A. Hussaini, "Advancing structural health monitoring: A vibration-based IoT approach for remote real-time systems," *Sensors and*

Actuators A: Physical, vol. 365, p. 114863, 2024, doi: https://doi.org/10.1016/j.sna.2023.114863.

[10] R. Kociszewski and W. Wojtkowski, "Remote Vibration Monitoring of Combustion Engines Utilising Edge Computing," *Electronics,* vol. 14, no. 11, p. 2118, 2025, doi: https://doi.org/10.3390/electronics14112118.

[11] A. H. Gomaa, "Maintenance 4.0: Optimizing Asset Integrity and Reliability in Modern Manufacturing," *Int. J. Inven. Eng. Sci.(IJIES),* vol. 12, pp. 18-26, 2025, doi: 10.35940/ijies.B1098.12020225.

[12] S. Chaturvedi, A. Parakh, and H. K. Verma, "Development of a wsn based data logger for electrical power system," 2019: Springer, pp. 72-83, doi: https://doi.org/10.1007/978-981-15-1384-8_7.

[13] A. Yasin, T. Y. Pang, C.-T. Cheng, and M. Miletic, "A roadmap to integrate digital twins for small and medium-sized enterprises," *Applied Sciences,* vol. 11, no. 20, p. 9479, 2021, doi: https://doi.org/10.3390/app11209479.

[14] M. I. Badranaya, J. Pratama, U. A. Salim, S. Suyitno, B. Arifvianto, and M. Mahardika, "A Method for Micro Powder Dispensing by Using DC Motor with a 2-Axis Vibration," *Applied Mechanics and Materials,* vol. 918, pp. 3-9, 2024, doi: https://doi.org/10.4028/p-pCY1mo.

[15] M. H. M. Ghazali and W. Rahiman, "An investigation of the reliability of different types of sensors in the real-time vibration-based anomaly inspection in drone," *Sensors,* vol. 22, no. 16, p. 6015, 2022, doi: https://doi.org/10.3390/s22166015.

[16] T. Leppänen, "Data visualization and monitoring with Grafana and Prometheus," 2021.

[17] R. Pallas-Areny and J. G. Webster, *Sensors and signal conditioning*. John Wiley & Sons, 2012.

[18] K. Mykoniatis, "A real-time condition monitoring and maintenance management system for low voltage industrial motors using internet-of-things," *Procedia Manufacturing,* vol. 42, pp. 450-456, 2020, doi: https://doi.org/10.1016/j.promfg.2020.02.050.

[19] J. R. Burnett and T. C. Lisk, "The future of employee engagement: Real-time monitoring and digital tools for engaging a workforce," in *International perspectives on employee engagement*: Routledge, 2021, pp. 117-128.

[20] K. A. Hossain, "Study on electromagnetic interference (EMI) and electromagnetic compatibility (EMC): sources and design concept for mitigation of EMI/EMC," *Journal of Liberal Arts and Humanities (JLAH),* vol. 4, no. 8, pp. 68-96, 2023.

JOURNAL OF AUTOMOTIVE AND MECHANICAL APPLIED TECHNOLOGY

Vol. 2 No. 1, 2025, pp. 76-83 https://journal.uny.ac.id/publications/jamat https://doi.org/10.21831/jamat.v2i1.1276

Testing of Design and Functionality of Front Suspension Arm in UNY Automotive Electric Vehicle for Individuals with Disabilities

Candra Kusuma Aditama[1], Muhammad Yusri Ismail[2], Ibnu Siswanto[3*]

[1]Department of Mechanical and Automotive Engineering, Faculty of Vocational, Universitas Negeri Yogyakarta, Kulon Progo, Yogyakarta 55652, Indonesia
[2]Faculty of Mechanical and Automotive Engineering Technology, Universiti Malaysia Pahang, Pekan, 26600, Malaysia
[3]Department of Automotive Engineering Education, Faculty of Engineering, Universitas Negeri Yogyakarta, Sleman, Yogyakarta 55281, Indonesia

*Corresponding author: ibnusiswanto@uny.ac.id

ARTICLE INFO

Article history:
Received 05.02.2025
Revised 28.02.2025
Accepted 27.03.2025

Keywords:
Safety Factor; Front Suspension Arm; Disabilities; Electric Vehicle

ABSTRACT

This study aims to evaluate the design and functionality of the front suspension arm in an electric vehicle specifically designed for users with disabilities. The research focuses on the lower arm component, analyzing its structural integrity through finite element analysis using ANSYS Student Version. The simulation was conducted under two loading conditions: 1300 N and 4800 N, representing different stress scenarios based on the vehicle's weight distribution. The safety factor analysis indicates that under a 1300 N load, the lower arm achieves a safety factor of 9.37, demonstrating high structural strength. Under an increased 4800 N load, the safety factor decreases to 2.54, which remains within the acceptable range (2.5–4.0) for static components subjected to dynamic loads. In terms of stress distribution, the simulation results indicate that the maximum stress is 39.51 MPa at a load of 1300 N. In contrast, it reaches 145.9 MPa at 4800 N. The displacement analysis reveals that the maximum deformation under 1300 N is 0.03023 mm, increasing to 0.1116 mm under 4800 N, indicating minimal structural deformation. Based on these findings, the lower arm suspension is deemed structurally safe and capable of withstanding the expected operational loads. These results offer valuable insights for the development of adaptive electric vehicles, ensuring their reliability and safety for users with disabilities.

1. Introduction

Land transportation serves as the primary mode of daily mobility for the Indonesian population. However, the continuous increase in fuel-powered vehicle usage poses a significant challenge due to the depletion of fossil fuel resources, which are non-renewable. Consequently, alternative solutions are required to ensure sustainable mobility without exacerbating existing issues [1].

In the context of globalization and industrialization, Indonesia must strategically leverage both challenges and opportunities to remain competitive on a global scale [2]. One of the emerging transportation alternatives is the electric vehicle, which was first introduced by Robert Anderson in Scotland between 1832 and 1839. However, during that period, fossil fuels were abundant and inexpensive, leading to a preference for fuel-powered vehicles over electric alternatives [3]. Electric vehicles operate using an electric motor powered by energy stored in rechargeable batteries. Given the rising fuel prices and increasing environmental concerns, electric vehicles have gained prominence as an energy-efficient and environmentally friendly transportation option, as they do not produce harmful emissions [4].

Simultaneously, accessibility to transportation remains a critical issue for individuals with disabilities. The term "disability" originates from "different ability," referring to individuals with distinct capabilities or specific needs. This terminology replaces "handicapped," which carries a negative connotation [5]. Disabilities are generally classified into three categories: physical disabilities, which involve impairments affecting bodily functions; mental disabilities, which pertain to limitations in cognitive and logical reasoning; and social disabilities, which manifest as difficulties in adapting to societal norms, regulations, and environmental conditions [6].

The development of electric vehicles designed specifically for individuals with disabilities aims to enhance mobility, particularly for those with physical impairments. These vehicles are designed as single-passenger units, offering wheelchair accessibility to accommodate users with mobility impairments. Currently, the development of electric vehicles for individuals with disabilities remains in the prototyping stage, serving as part of ongoing technological advancements. The selection of suspension systems and materials represents a critical aspect of vehicle design, necessitating a thorough review of existing literature to inform the engineering and innovation processes in the field of automotive technology [7, 8]. This study focuses on the design and development of the upper and lower control arms for the front suspension system of an electric vehicle prototype designed for individuals with disabilities, developed at Universitas Negeri Yogyakarta (UNY). The research process follows a structured and systematic approach, requiring interdisciplinary collaboration to ensure the successful completion of this project [9].

2. Methodology

This research employs the ADDIE development method, which consists of five main stages: Analysis, Design, Development, Implementation, and Evaluation. This method was chosen because it follows a systematic and procedural approach, ensuring that the designed product meets the specified requirements while minimizing the risk of failure in the development process [10, 11].

2.1 Analysis

At this stage, an analysis is conducted on the design requirements of the electric vehicle for people with disabilities, including factors that influence the design of the front suspension. Additionally, observations and literature studies related to vehicle design for people with disabilities are conducted to gather relevant references [12]. This section also includes simple calculations using basic static mechanics equations [13] based on Newton's Third Law to determine the load used in the design process, where

$$F\ action = f\ Reaction \tag{1}$$

2.2 Design

After the design requirements and specifications are determined, the design phase is carried out using Autodesk Inventor 2021 student version. This process involves creating a three-dimensional model of the front suspension's upper and lower arm components, as well as conducting an initial simulation to determine the resulting stress, which serves as a reference for material selection.

2.3 Development

The designed model is then tested using ANSYS 2022 student version to analyze the material strength and stress distribution on the suspension components. The simulation is conducted with loading conditions based on the vehicle's weight calculations to ensure the design's strength and safety. If the simulation results indicate potential structural failure, the design will be revised before proceeding to the next stage.

2.4 Implementation

After the design is approved based on the simulation results, the fabrication process is carried out to realize the design. The material used for manufacturing the components is steel, chosen for its ease of modification and high toughness. The fabrication process is conducted using MIG welding, which is selected for its precision and minimal impact on material properties, ensuring dimensional accuracy according to the design specifications.

2.5 Evaluation

The final stage of this research involves evaluating the fabricated components, which includes testing the vehicle to assess the suspension's performance under operational conditions. This evaluation is qualitative and subjective, meaning no quantitative measurements are taken; instead, a descriptive analysis is conducted to determine whether the suspension functions properly or not [14].

3. Result and Discussion

Fig. 1 shows the dimensions of the designed vehicle and the modified front suspension components. Based on these dimensions and assuming a total vehicle weight of 412 kg, the load distribution on each wheel is calculated using Equation 1. The results indicate that the front suspension supports a load of 248.95 kg, while the rear supports 81.525 kg. This means that each front wheel bears a load of 128.475 kg. Thus, in the design process, a 1300 N load is used, which is a rounded conversion of the load supported by the front wheels.

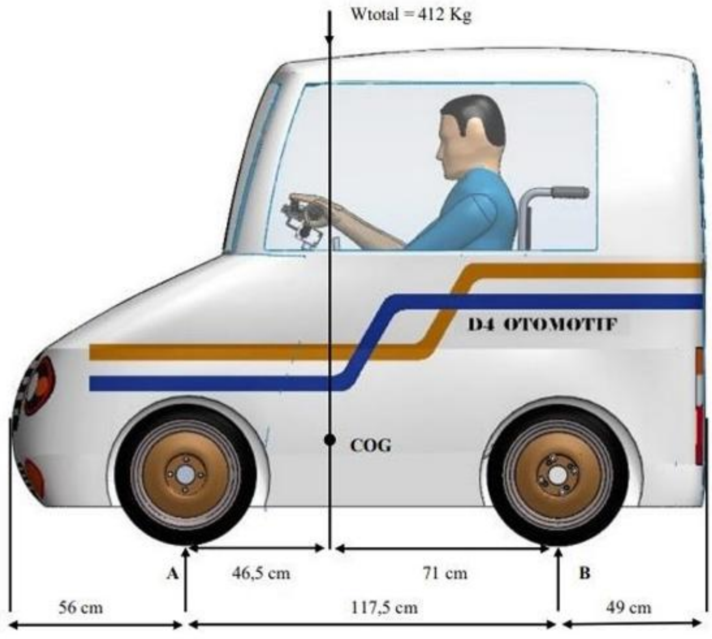

Figure 1. Dimensions of the design vehicle.

Next, the upper arm and lower arm designs used in the vehicle suspension system are shown in Fig. 2. The dimensions have been adjusted to meet the vehicle's requirements, taking into account both functionality and ease of fabrication. The design follows a simple concept that allows for manufacturing using basic tools, thereby reducing production costs. Additionally, ease of installation is a key factor considered in shaping the design.

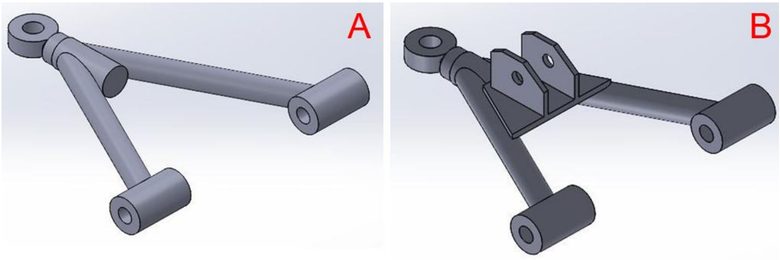

Figure 2. Design of a) upper arm and b) lower arm

To ensure that the lower arm can withstand the vehicle's load, an analysis was conducted using Ansys Student Version. The simulation model used in this analysis is illustrated in Fig. 3. The analysis includes a safety factor calculation, which serves as a benchmark for determining whether the design is safe under load testing conditions. The testing was performed under two loading scenarios: 1300 N and 4800 N. This is based on the fact that each front suspension side supports 128.475 kg or 1284.75 N.

According to the analysis results, under a 1300 N load, the lower arm exhibits a safety factor of 9.37, indicating excellent resistance to the applied forces. Meanwhile, under a higher load of 4800 N, the safety factor decreases to 2.54, which still falls within the safe range of 2.5 to 4.0, commonly used as a guideline for static components under dynamic loads [15]. Thus, it can be concluded that the lower arm can safely support the vehicle's weight, even up to a maximum load of 4800 N. The safety factor visualization from this analysis is presented in Fig. 4.

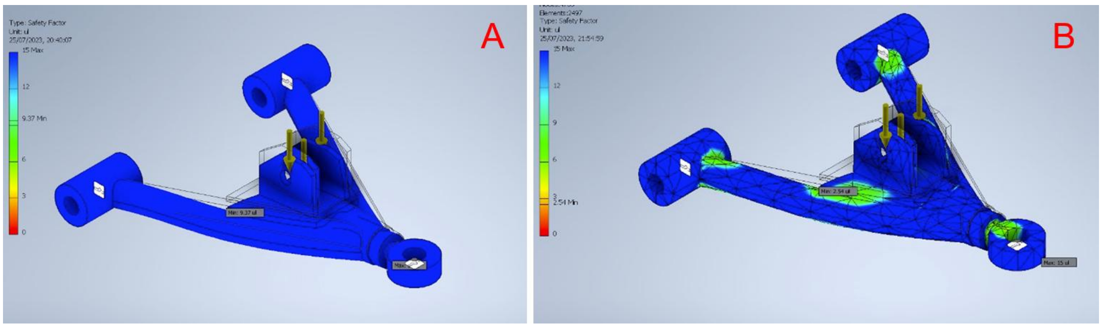

Figure 3. Lower arm safety factor simulation of a) 1300 N and b) 4800 N

Besides safety factor analysis, stress analysis was also performed on the lower arm to evaluate the stress distribution caused by loading. The simulation results indicate that under 1300 N, the minimum stress is 0.04 MPa, while the maximum stress reaches 39.51 MPa. When the load increases to 4800 N, the minimum detected stress is 0.2 MPa, while the maximum stress rises to 145.9 MPa. The stress distribution on the lower arm under both loading conditions is shown in Fig. 5.

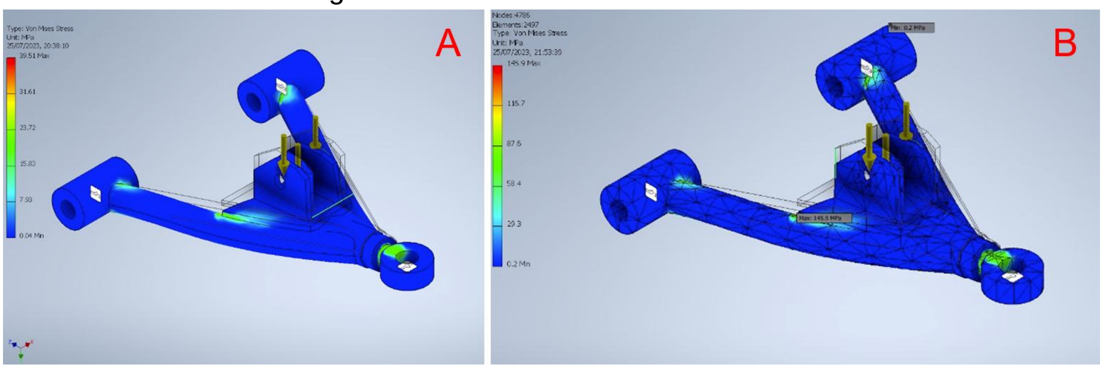

Figure 4. Lower arm stress simulation of a) 1300 N and b) 4800 N

Additionally, a displacement analysis was conducted to determine the magnitude of deformation in the lower arm under load. The results show that at a load of under 1300 N, the maximum displacement is 0.03023 mm, while the minimum remains 0 mm. When the load increases to 4800 N, the maximum displacement rises to 0.1116 mm. Despite this increase, the displacement values remain within a safe range that does not cause structural failure in the lower arm. The displacement visualization is displayed in Fig. 6, and the complete simulation results are summarized in Table 1.

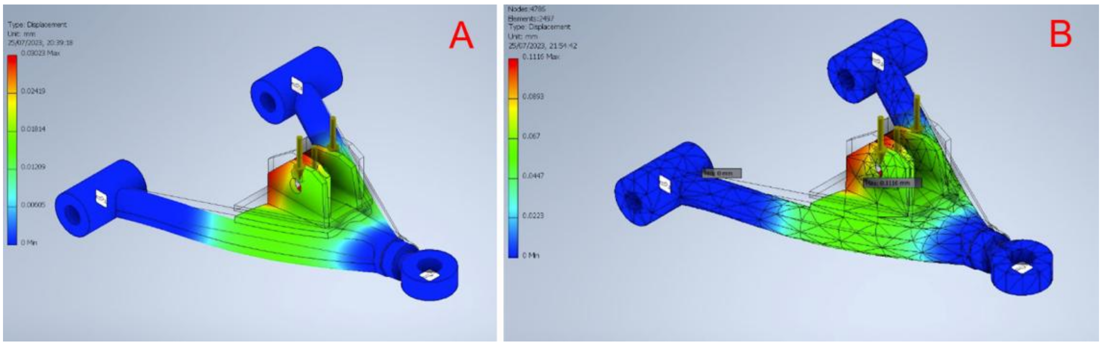

Figure 5. Lower arm displacement simulation of a) 1300 N and b) 4800 load

Table 1. Simulation result

Aspect	1300 N	4800 N
Safety factor	9.37	2.54
Max stres (MPa)	39.51	145.9
Max displacement (mm)	0.030	0.11

Based on the analysis, it can be concluded that the designed lower arm has a high level of safety and can effectively support the vehicle's weight. The obtained safety factor confirms that the component is safe for use. At the same time, stress and displacement analyses indicate that the design functions as intended, with no excessive deformation. However, to verify that the component is not only structurally strong in theory but also functions effectively in real conditions, functional testing was conducted on both the upper arm and lower arm [16].

The functional tests aimed to evaluate the ability of the component to control wheel movement, support the knuckle, support the shock absorber, and adjust the camber angle [17]. The first test examined whether the upper arm and lower arm could properly control wheel movement. The vehicle was subjected to internal shocks, causing the wheels to move up and down. The results confirmed that both components effectively controlled wheel movement smoothly without obstruction or mechanical issues.

Next, a knuckle support test was conducted. The knuckle was installed and directly connected to the wheel, then secured using the upper arm and lower arm with bolts [18]. The results showed that these components provided a strong grip on the knuckle, enabling stable wheel movement. This indicates that the design is suitable for firmly supporting the knuckle, as illustrated in Fig. 6.

The next test ensured that the lower arm could adequately support the shock absorber. In the vehicle's suspension system, the lower part of the shock absorber is connected to the lower arm, while the upper part is attached to the vehicle chassis [19]. The test involved applying internal load shocks to verify whether the shock absorber could absorb impacts properly. The results showed that the shock absorber functioned optimally, and the lower arm supported it without deformation or performance issues. The test illustration is presented in Fig. 6.

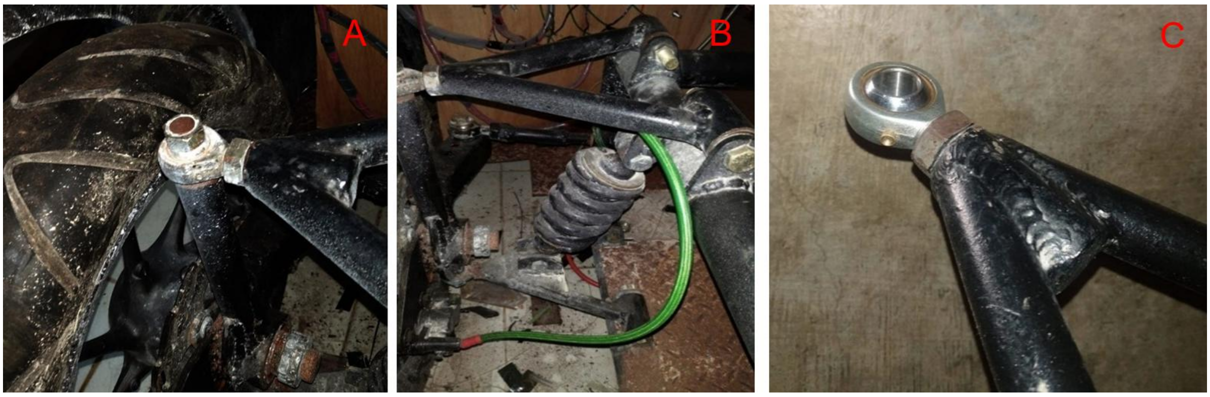

Figure 6. Design testing of a) Knuckle support test, b) Suspension test and c) camber angle test

The final test evaluated the upper arm and lower arm in adjusting the camber angle, which is crucial for vehicle stability during motion. The test involved rotating the bearing rod ends to adjust the length of the upper and lower arms, thereby modifying the camber angle as needed [20]. The results confirmed that the bearing rod ends functioned effectively, allowing optimal suspension geometry adjustments. The test results are shown in Fig. 6.

From all the tests conducted, it can be concluded that the upper arm and lower arm designs applied to UNY's automotive electric vehicle for disabled individuals meet the required functional standards. These components are not only structurally strong but also function effectively in controlling wheel movement, supporting the knuckle and shock absorber, and allowing precise camber angle adjustments. Therefore, this suspension design can be effectively used to enhance vehicle comfort and stability in various operating conditions.

4. Conclusion

The results of the research show that the electric vehicle prototype's upper and lower suspension arms are strong enough and safe enough to withstand dynamic loading conditions. The lower arm component shows a substantial safety margin in the finite element analysis conducted using ANSYS. The safety factor is 9.37 under a 1300 N load and 2.54 with a 4800 N load. All of these numbers are within the safe range for components that are dynamically stressed, thus it looks like the structure can handle both typical and exceptional loads. There would be no structural collapse under those conditions because the associated stress values, 39.51 MPa for 1300 N and 145.9 MPa for 4800 N, are significantly lower than the yield strength of the chosen material.

The suspension unit is structurally sturdy, and it also serves its functional purpose well. The capacity of the upper and lower arms to sustain important suspension components, like the knuckle and shock absorber, was evaluated. These parts keep the knuckle in position and make sure the shock absorber works properly, so it can absorb energy from bumps in the road, according to the tests. Also, you may change the camber angle with the bearing rod ends and the suspension system is flexible enough to adapt the alignment. Electric vehicles made for people with impairments benefit greatly from this function because it improves the vehicle's handling and stability. The design's simplicity is another noteworthy achievement. It was with this ease of fabrication and installation in mind that the suspension arms were devised. In addition to facilitating possible manufacturing scalability, this method simplifies and lowers the cost of production. Little distortion seen in the simulations proves that performance is unaffected by the design's seeming simplicity. The greatest displacement measured was a respectable 0.03023 mm under a 1300 N loading and a somewhat higher 0.1116 mm under a 4800 N loading, both of which are well within the allowable tolerance limit.

References

[1] B. P. Resosudarmo, F. Jotzo, A. A. Yusuf, and D. A. Nurdianto, "Challenges in mitigating Indonesia's CO2 emission: The importance of managing fossil fuel combustion," 2011, doi: 10.22004/ag.econ.249531.

[2] U. Salam, S. Lee, V. Fullerton, Y. Yusuf, S. Krantz, and M. Henstridge, "Indonesia case study: Rapid technological change–challenges and opportunities," *Pathways for Prosperity Commission Background Paper Series,* pp. 2019-09, 2018.

[3] D. J. Soeder, "Replacing Fossil Fuels," in *Energy Futures: The Story of Fossil Fuel, Greenhouse Gas, and Climate Change*: Springer, 2025, pp. 143-183.

[4] C. M. Costa, J. Barbosa, Castro, H. Castro, R. Gonçalves, and S. Lanceros-Méndez, "Electric vehicles: To what extent are environmentally friendly and cost effective?–Comparative study by european countries," *Renewable and Sustainable Energy Reviews,* vol. 151, p. 111548, 2021, doi: https://doi.org/10.1016/j.rser.2021.111548.

[5] S. Linton, "Reassigning meaning," in *Beginning with Disability*: Routledge, 2017, pp. 20-27.

[6] A. P. Kinzig *et al.*, "Social norms and global environmental challenges: the complex interaction of behaviors, values, and policy," *BioScience,* vol. 63, no. 3, pp. 164-175, 2013, doi: https://doi.org/10.1525/bio.2013.63.3.5.

[7] E. A. Etukudoh, F. O. Usman, V. I. Ilojianya, C. D. Daudu, A. A. Umoh, and K. I. Ibekwe, "Mechanical engineering in automotive innovation: A review of electric vehicles and future trends," *International Journal of Science and Research Archive,* vol. 11, no. 1, pp. 579-589, 2024, doi: https://doi.org/10.30574/ijsra.2024.11.1.0081.

[8] F. Khan *et al.*, "Advances of composite materials in automobile applications–A review," *Journal of Engineering Research,* 2024, doi: https://doi.org/10.1016/j.jer.2024.02.017.

[9] E. O. Nwulu, T. Y. Elete, K. O. Omomo, O. A. Akano, and O. V. Erhueh, "The importance of interdisciplinary collaboration for successful engineering project completions: A strategic framework," *World Journal of Engineering and Technology Research,* vol. 2, no. 3, pp. 48-56, 2023, doi: 10.53346/wjetr.2023.2.3.0048.

[10] D. Adriani, P. Lubis, and M. Triono, "Teaching material development of educational research methodology with Addie Models," 2020, doi: http://dx.doi.org/10.4108/eai.4-12-2019.2293793.

[11] H. Crompton *et al.*, "Examining technology use within the ADDIE framework to develop professional training," *European Journal of Training and Development,* vol. 48, no. 3/4, pp. 422-454, 2024, doi: https://doi.org/10.1108/EJTD-12-2022-0137.

[12] B. E. Dicianno *et al.*, "Systematic review: Automated vehicles and services for people with disabilities," *Neuroscience letters,* vol. 761, p. 136103, 2021, doi: https://doi.org/10.1016/j.neulet.2021.136103.

[13] J. F. Doyle, *Static and dynamic analysis of structures: with an emphasis on mechanics and computer matrix methods*. Springer Science & Business Media, 2012.

[14] C. Kennedy, "Two sources of subjectivity: Qualitative assessment and dimensional uncertainty," *Inquiry,* vol. 56, no. 2-3, pp. 258-277, 2013, doi: https://doi.org/10.1080/0020174X.2013.784483.

[15] A. Widyianto, A. S. Baskoro, and G. Kiswanto, "Design and Analysis of Orbital Pipe Welding Prototype for Piping System Welding Applications," *Journal of Automotive and Mechanical Applied Technology,* vol. 1, no. 1, pp. 11-23, 2024, doi: 10.21831/jamat.v1i1.797.

[16] N. Anuar *et al.*, "Development of an Endurance Test Procedure for Vehicle Control Arm through Vehicle Dynamic Testing and Load Transfer Analysis," *Automotive Experiences,* vol. 7, no. 3, 2024, doi: https://doi.org/10.31603/ae.12561.

[17] T. Hadland, "Wheels and shock absorption," in *Routledge Companion to Cycling*: Routledge, 2022, pp. 108-117.

[18] S. Yadav, R. K. Mishra, V. Ansari, and S. B. Lal, "Design and analysis of steering knuckle component," *Int. J. Eng. Res,* vol. 4, 2016, doi: 10.23883/IJRTER.2018.4092.MYRIK.

[19] M. S. A. Pachapuri, R. G. Lingannavar, N. K. Kelageri, and K. K. Phadate, "Design and analysis of lower control arm of suspension system," *Materials Today: Proceedings,* vol. 47, pp. 2949-2956, 2021, doi: https://doi.org/10.1016/j.matpr.2021.05.035.

[20] Q. Li, X. Chen, T. Zhang, S. Chen, and J. Gu, "Experimental research on cage dynamic characteristics of angular contact ball bearing," *Mechanics & Industry,* vol. 20, no. 2, p. 204, 2019, doi: https://doi.org/10.1080/10402004.2020.1790706.

JOURNAL OF AUTOMOTIVE AND MECHANICAL APPLIED TECHNOLOGY

Vol. 2 No. 1, 2025, pp. 84-92 https://journal.uny.ac.id/publications/jamat https://doi.org/10.21831/jamat.v2i1.1342

Prototype of an Adaptive Wiper System for Electric Vehicles for Disabled Users Using a Servo Motor

Raihan Bayu Nugroho[1], I Wayan Warsita[2], I Wayan Adiyasa[3*]

[1]Department of Mechanical and Automotive Engineering, Faculty of Vocational, Universitas Negeri Yogyakarta, Kulon Progo, Yogyakarta 55652, Indonesia
[2]Graduate School of Mechanical Engineering, University of Ulsan, DaeHak-ro 93, Nam-gu, Ulsan 44610, South Korea
[3]Department of Automotive Engineering Education, Faculty of Engineering, Universitas Negeri Yogyakarta, Sleman, Yogyakarta 55281, Indonesia

*Corresponding author: iwayanadiyasa@uny.ac.id

ARTICLE INFO

Article history:
Received 25.02.2025
Revised 20.03.2025
Accepted 12.04.2025

Keywords:
Servo Motor; Electric Vehicle; Wiper System; Disabilities

ABSTRACT

This study presents the design and implementation of a prototype wiper system using a servo motor, specifically developed for electric vehicles designed for persons with disabilities. The system is structured through several stages, including the creation of a wiring diagram, the development of a control system based on an Arduino Uno microcontroller, and the integration of key components such as a 12V battery, a three-position switch, a step-down LM2596 module, and an RDS3239 servo motor. The control logic enables two-speed wiping modes low and high regulated by user input via the switch. Electrical testing demonstrated that the current drawn by the system was 0.26 A at low speed and 0.37 A at high speed, with corresponding power consumption of 3.12 W and 4.44 W, respectively. These values fall within safe operating limits, indicating energy efficiency suitable for electric vehicle applications. Motion testing showed that the system achieved 30 wipes per minute at low speed and 60 wipes per minute at high speed, with the high-speed mode meeting the minimum functional criteria set by national standards. Angular deviation analysis further revealed that increased speed slightly impacted sweep precision, though still within acceptable tolerances. The results indicate that the developed system not only performs effectively in varying operational conditions but also offers energy-efficient and responsive functionality. This makes it a viable solution for adaptive and accessible mobility technologies in electric vehicles for persons with disabilities.

1. Introduction

People with disabilities are closely linked to social life in society. They are often identified by various terms such as "people with disabilities," "differently-abled," "special needs," and "individuals with limitations." The term "differently-abled" refers more to physical limitations, such as the loss of certain body parts that cause disability [1]. Each individual with a disability has their own specific limitations, which are often referred to with the prefix "tuna" in Indonesian, meaning "lack" or "absence." Examples include "tunanetra" (visual impairment), "tunagrahita" (intellectual disability), "tunalaras" (emotional or behavioral disorders), and "tunadaksa" (physical disabilities) [2].

People with disabilities are often viewed as second-class citizens, leading to discriminatory actions against them [3]. According to Law No. 19 of 2011 on the Ratification of the Rights of Persons with Disabilities, individuals with disabilities are those who have long-term physical, mental, intellectual, or sensory limitations that hinder them from participating fully and effectively in society on an equal basis with others. It is important to note that the term "differently-abled" does not imply incapacity, but rather emphasizes their unique ways of performing activities according to their limitations [4]. Therefore, it is crucial for society to understand and appreciate these differences and provide opportunities for people with disabilities to actively participate in social life and communities without discrimination [5].

Every citizen has the right to receive equal rights and opportunities, including the right to rehabilitation, education, employment, and career development. However, discriminatory attitudes still exist in society, often leading to unequal access to education and difficulty for people with disabilities in obtaining employment [6]. Employment opportunities for them are still limited and do not match their number in each region. Additionally, there is a lack of entrepreneurship training and skill development support tailored to their needs. According to Law No. 4 of 1997, Article 14, persons with disabilities are entitled to occupy at least 1% of positions in companies with more than 100 employees [7].

The government has a responsibility to ensure equal rights for people with disabilities, especially in transportation. Transportation is a basic need in everyday life, and various modes of public and private transport must be accessible to everyone. To support inclusive public services, the government regulates the accessibility rights of people with disabilities through various regulations, including the 2016 Disability Rights Law. The main challenges in this area include the adequacy of service providers, protection of rights, and public service accessibility. Inclusive transportation becomes a crucial step toward building a society that supports the participation of all individuals [8].

Transportation plays a vital role in the economy, enabling independence in daily activities such as traveling for education, work, or family needs. To enhance accessibility, special driver's licenses have been introduced for people with disabilities. One notable innovation is the modification of two-wheeled motorcycles into three-wheeled versions designed for individuals with physical disabilities, providing safer and more comfortable travel.

The term "tunadaksa" refers to individuals with physical limitations—whether congenital or acquired through accidents or disasters—that hinder their physical mobility. Although the government has issued regulations such as Law No. 4 of 1997, Article 6, to support their rights, the availability of public facilities that meet their needs is still limited. Wheelchair users often face difficulties accessing public transportation due to inadequate infrastructure, which not only restricts their mobility but also increases transportation costs. Mobility aids such as wheelchairs, crutches, and other assistive devices are essential, but their availability and suitability vary among individuals. Therefore, it is essential for the government and related parties to improve transportation accessibility to ensure equal opportunities for people with disabilities. This will enhance their independence, quality of life, and social inclusion [9].

In response to this, a team of students from Universitas Negeri Yogyakarta plans to develop a special vehicle for people with disabilities. This electric vehicle, powered by an electric motor, is designed to provide safe, comfortable, energy-efficient, and environmentally friendly mobility. The production process includes the creation of a chassis, installation of suspension, steering system, braking system, wheels, body, interior, and electrical system planning. One crucial component of this system is the wiper mechanism, which plays an essential role in maintaining visibility during rainy conditions. A well-functioning wiper is critical for driver safety, ensuring clear vision through the windshield and preventing accidents caused by limited visibility.

This study aims to enhance the safety and comfort of drivers with disabilities. The wiper system is crucial for maintaining visibility by removing rainwater and dirt from the windshield. Without this system, driving in the rain would pose significant safety risks. Therefore, before proceeding with the wiper system's construction, a detailed design must be developed, followed by testing each component to ensure optimal performance.

2. Methodology

2.1 Development Method

The development of the servo motor system for electric vehicles for disabled individuals begins with system design based on user-specific needs and the functional analysis of the servo motor in driving the wiper mechanism. This development process consists of several main stages:

1. Needs Identification
   In the initial stage, user needs are identified for disabled individuals who require a wiper system that can be easily controlled. These needs include a responsive servo motor control system and a rain sensor capable of accurately detecting rain intensity.
2. System Design
   The system design uses a microcontroller as the controller unit, with a rain sensor integrated to detect water presence on the windshield, triggering the servo motor to activate the wiper. The design prioritizes ease of operation for disabled users and energy efficiency.
3. Component Selection
   The components are selected based on quality and long-term reliability. The chosen components include a servo motor with appropriate torque and speed, a rain sensor that works well under various weather conditions, and a microcontroller with flexible programming capabilities.
4. Prototype Development and Testing
   The prototype is developed by assembling all components into a system setup, followed by testing in relevant scenarios. The prototype is tested to ensure that the servo motor functions correctly and responds to the rain sensor's signals.

2.2 Material and setup

This section describes the specifications of the materials and the experimental setup used in the study.

1. Servo Motor
   The servo motor used in the experiment is a high-torque type designed to drive the wiper on the electric vehicle. This motor is chosen for its precision and ability to be controlled by PWM (Pulse Width Modulation) signals from the microcontroller. The specifications of the servo motor used are as follows: Torque: 10 kg·cm, Speed: 60 degrees per second and Power: 5V.
2. Rain Sensor
   The rain sensor used is designed to detect the presence of water on the surface of the windshield and send a signal to the microcontroller to activate the servo motor. This sensor operates based on changes in resistance that occur when water contacts the sensor surface. The specifications of the rain sensor used are as follows: Type: Resistive-based sensor, Operating Voltage: 5V and Sensitivity: Capable of detecting rain intensity from light to heavy.
3. Microcontroller
   The microcontroller used in the system is an Arduino Uno, equipped with input/output pins to receive signals from the rain sensor and control the servo motor. The microcontroller is also programmed to adjust the servo motor's speed and movement duration based on the detected rain intensity.

4. Power Supply
   The power supply used to operate the system is a 12V Li-ion battery, commonly used in electric vehicles. This battery is chosen for its efficiency in providing stable power to the system components.

2.3 Experimental Procedure

This section describes the specifications of the materials and the experimental setup used in the study. The experimental procedure is designed to test the performance of the servo motor system controlled by the rain sensor under actual conditions. The stages of the experiment are as follows:

1. Experimental Setup Preparation
   All components, including the servo motor, rain sensor, and microcontroller, are mounted on the electric vehicle according to the design specified in the material and setup section. All connections between the devices are checked to ensure no disruptions or malfunctions in the system.
2. Rain Sensor Responsiveness Test
   In this stage, the rain sensor is tested to ensure it accurately detects the presence of water. The sensor is tested under various conditions, from light rain to heavy downpours, to observe how the system responds to different levels of rain intensity. The microcontroller connected to the sensor sends signals to the servo motor to move the wiper accordingly.
3. Servo Motor Performance Test
   Once the rain sensor is functioning correctly, the servo motor's performance in driving the wiper is tested. The motor is evaluated under various speed and movement duration conditions, as well as different levels of rain intensity detected by the sensor. The motor's reliability is measured based on its response time and the accuracy of its movement in driving the wiper.
4. Result Analysis
   The results of the experiment will be analyzed to assess the system's effectiveness in controlling the wiper motor based on the rain detection sensor. The analysis includes measuring the motor's response time, movement accuracy, and overall system performance under different rain conditions. The experimental data obtained will be used to refine the system and improve its efficiency.

3. Result and Discussion

3.1 System Design Process

The design process of the wiper system for electric vehicles intended for persons with disabilities was carried out in several stages, starting from the development of a wiring diagram, control system design, to the integration of all components into a functional system. The wiring diagram was created using the Draw.io application, which was utilized to illustrate the connectivity between key components such as the 12V battery, three-position switch, servo motor, and LM2596 step-down module. The wiring configuration is shown in Fig. 1.

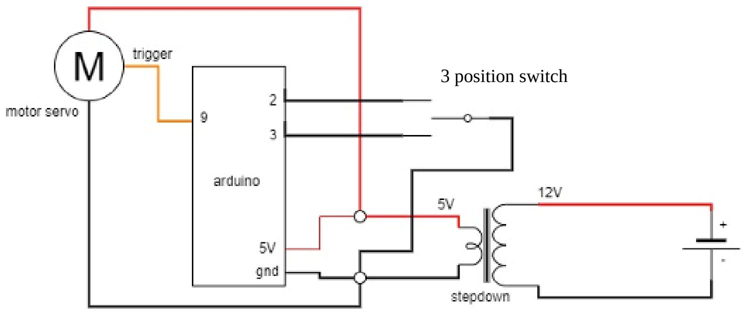

Figure 1. Wiring system diagram

The next step involved designing a control system based on the Arduino platform. The switch circuit was designed as the primary input to regulate the speed modes of the wiper sweep. Signals from the switch were received by the Arduino Uno to determine the motor servo movement instructions. The voltage from the 12V battery was stepped down using the LM2596 module to 5V, which matches the operating requirements of both the Arduino and the servo motor. The RDS3239 servo motor, acting as the actuator, was configured to produce sweeping angles based on the commands programmed into the Arduino logic [10].

Figure 2. Complete system assembly

Once each circuit was tested individually, all the subsystems were integrated into a single, unified circuit. System testing was conducted to ensure that communication among components functioned as intended. To support system performance, the Arduino program was carefully structured to enable the servo motor to operate at two distinct speed modes depending on the input from the switch [11]. The system's reliability heavily relied on the accuracy of the wiring and the correctness of the programming syntax. The complete system assembly is shown in Fig. 2.

3.2 Voltage and Current Testing

The primary objective of the current testing was to measure the electric current flowing through the wiper system under two different speed modes. The measured current serves as a key indicator to evaluate whether the electrical system can adequately support the operation of the servo motor, and to ensure that no overcurrent conditions or system failures occur due to excessive current. The test results showed that at low speed, the current drawn by the wiper system was 0.26 A, whereas at high speed, the current increased to 0.37 A. This increase in current corresponds to the higher power demand required by the motor at higher speeds [12]. In other words, the higher the operating speed, the greater the current needed to allow the motor to function optimally [13].

Table 1. Current and voltage test result

No	Data	Voltage (V)		Voltage Stepdown (V)	Current (A)	Power (W)	Resistance (Ω)
		Reference	Actual				
1	Low Speed	11–12	12	5	0.26	3.12	0.8
2	High speed	11–12	12	5	0.37	4.44	1.0

Referring to Table 1, it was found that at low speed, the wiper motor required 3.12 Watts of power, while at high speed, the power demand increased to 4.44 Watts. This difference in power consumption aligns with the typical behavior of motors, which require more energy to operate at higher speeds. It also indicates that the wiper system is capable of adjusting its energy consumption based on the required operating speed.

It is important to note that at both speed levels, the power consumption remained within safe and efficient limits. At low speed, the required power was relatively small, allowing the motor to operate efficiently without placing excessive load on the vehicle's electrical system [14]. At high speed, although the power requirement was higher, it was still within acceptable limits since the system is designed to deliver optimal performance under more demanding weather or operational conditions. This power test also demonstrates that the servo motor used in this system can operate across a fairly wide power range, providing flexibility in energy management for the vehicle. Therefore, the system not only performs effectively but also emphasizes energy efficiency, which is crucial for electric vehicles especially those designed for people with disabilities, where power optimization is a key consideration.

3.3 Wiper Movement Testing

The testing focused on evaluating the number of wiper blade sweeps or back-and-forth motions per minute. The measurement was conducted under two different speed modes low and high with the objective of assessing the performance of the servo motor-based electric wiper system. The number of sweeps is a crucial parameter as it directly reflects the system's effectiveness in clearing the windshield or wiping surface from water or debris.

The test results showed that at high speed, the system was able to produce 60 wiper sweeps per minute, while at low speed, it generated only 30 sweeps per minute. These tests were conducted using an acrylic sheet as a substitute for automotive glass, considering practicality and safety during simulation. However, the use of acrylic may introduce higher friction and load on the motor compared to standard automotive glass.

When compared to the minimum requirement set by the Indonesian National Standard (SNI), which stipulates at least 45 sweeps per minute, it can be concluded that the wiper system in high-speed mode has met the functional feasibility criteria. The servo motor used provided sufficient torque and rotational speed to produce fast, stable, and responsive movement. This indicates that the system has strong potential for direct implementation in electric vehicles for people with disabilities as a reliable windshield cleaning solution [15].

On the other hand, the low-speed mode, which achieved only 30 sweeps per minute, did not meet the minimum regulatory threshold. However, this condition is still technically acceptable, given that the low-speed mode is typically used under light rain conditions or as an energy-saving option in electric vehicles. The slower motion also tends to be smoother and does not place excessive load on the electrical system. Therefore, although it falls below the standard limit, this mode remains relevant in terms of ergonomics and energy efficiency [16].

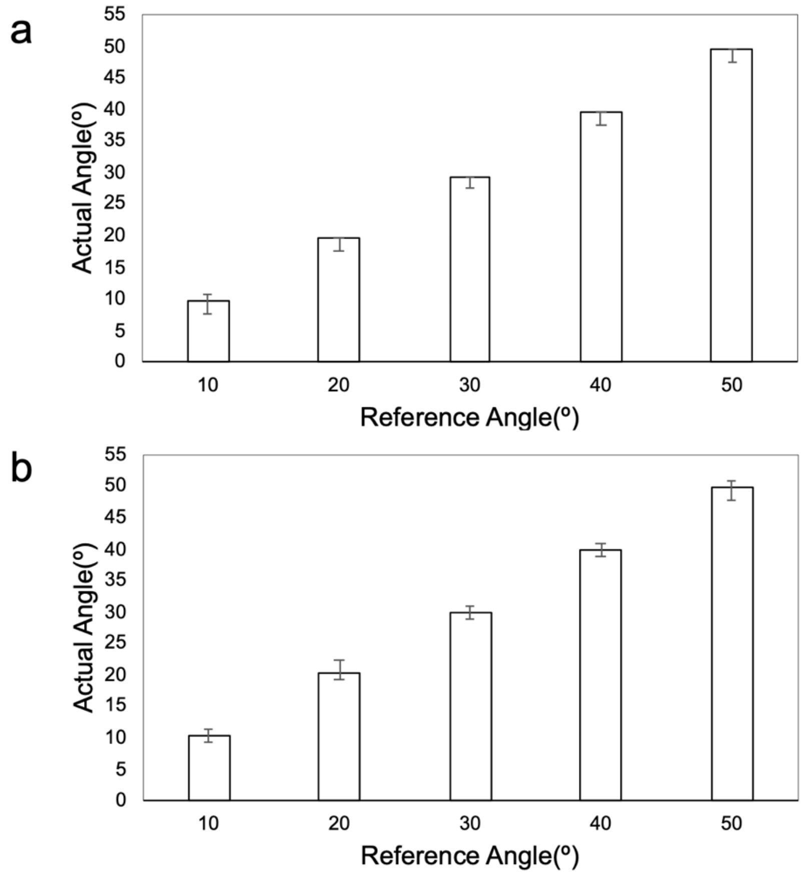

Figure 3. the measurement angel of wiper at: a) ow speed and b) High speed

Furthermore, the measurement results of the wiper sweep angles for each speed mode are illustrated in Fig. 3. For low-speed operation, the average angles observed were 10.3°, 20.4°, 29.9°, 39.9°, and 49.7°. These values show a deviation of approximately ±0.4° from the target angles of 10°, 20°, 30°, 40°, and 50°, respectively. In contrast, at high-speed operation, the measured angles were 9.7°, 19.5°, 29.4°, 39.5°, and 49.6°, with a deviation of about ±0.5°. Based on these measurements, it can be observed that higher wiper speeds tend to result in greater angular deviations. This finding indicates a trade-off between speed and motion accuracy, as the deviation values increase along with the wiper's operating speed [17].

4. Conclusion

The development of a servo motor-based wiper system for electric vehicles designed for individuals with disabilities has been carried out through a structured engineering approach, encompassing system design, control circuit development, and component integration. The system employs an Arduino Uno microcontroller to interpret inputs from a three-position switch, thereby regulating the motion of the RDS3239 servo motor. A step-down voltage module (LM2596) ensures appropriate voltage conversion from a 12V power supply to the 5V required by the control and actuator components. Current testing results indicate that the system operates within a safe and efficient electrical range. At low-speed operation, the system draws a current of 0.26 A, increasing to 0.37 A at high speed. Corresponding power consumption levels are 3.12 W and 4.44 W, respectively, which reflect the increased energy demand associated with higher mechanical output. These values remain within acceptable limits, confirming the system’s electrical efficiency and safety.

Kinematic performance was evaluated based on the number of wiper strokes per minute. At high speed, the system achieved 60 strokes per minute, thereby meeting the minimum performance threshold defined by the Indonesian National Standard (SNI). In contrast, the low-speed mode resulted in 30 strokes per minute. Although this value falls below the regulatory minimum, it remains functionally acceptable for light rainfall conditions or energy-saving applications. Additionally, angular displacement measurements revealed minimal deviation, with an average variance of ±0.4° at low speed and ±0.5° at high speed, indicating the system's capability to maintain accurate and stable actuation under varying operational conditions. In conclusion, the proposed wiper system demonstrates functional viability, electrical safety, and mechanical reliability. Its performance characteristics suggest suitability for implementation in electric vehicles for individuals with disabilities, where both energy efficiency and functional adaptability are critical. Future development may focus on system optimization, waterproofing, and extended durability testing to further enhance the reliability and practicality of the system in real-world scenarios.

Conflict of interest

The authors declare that they have no conflict of interest.

References

[1] M. M. Sefotho and P. L. Leshota, "Being differently abled: Disability through the lens of hierarchy of binaries and Bitso-lebe-ke Seromo," *African Journal of Disability,* vol. 9, no. 1, pp. 1-7, 2020.

[2] R. Stoutjesdijk, E. M. Scholte, and H. Swaab, "Special needs characteristics of children with emotional and behavioral disorders that affect inclusion in regular education," *Journal of emotional and behavioral disorders,* vol. 20, no. 2, pp. 92-104, 2012, doi: https://doi.org/10.1177/1063426611421156.

[3] A. Waldschmidt and M. Sépulchre, "Citizenship: reflections on a relevant but ambivalent concept for persons with disabilities," *Disability & Society,* vol. 34, no. 3, pp. 421-448, 2019, doi: https://doi.org/10.1080/09687599.2018.1543580.

[4] A. de Beer, L. Naudé, and L. Nel, "From disabled to differently abled: A psychofortological perspective on first-year students living with disability," *Indo-Pacific Journal of Phenomenology,* vol. 23, no. 1, p. e2222938, 2023, doi: https://doi.org/10.1080/20797222.2023.2222938.

[5] G. Akyurek and G. Bumin, "Community participation in people with disabilities," *Occupational therapy-occupation focused holistic practice in rehabilitation. Croatia: Intech,* pp. 81-107, 2017.

[6] K. Vornholt *et al.*, "Disability and employment–overview and highlights," *European journal of work and organizational psychology,* vol. 27, no. 1, pp. 40-55, 2018, doi: https://doi.org/10.1080/1359432X.2017.1387536.

[7] P. Thornton and N. Lunt, "Employment policies for disabled people in eighteen countries: A review," 1997.

[8] A. E. Dingil, "Fostering Inclusive Urban Transportation in Planning and Policy-Making: An Umbrella Review using ALARM Methodology," *Sustainable Futures,* p. 100420, 2024, doi: https://doi.org/10.1016/j.sftr.2024.100420.

[9] J. McClure and C. Leah, "Is independence enough? Rehabilitation should include autonomy and social engagement to achieve quality of life," *Clinical Rehabilitation,* vol. 35, no. 1, pp. 3-12, 2021, doi: https://doi.org/10.1177/0269215520954344.

[10] N. K. Ndwiga, "Design and Construction of A Microcontroller-Based Five Degree of Freedom Robotic Arm Using Servo Motors," *Kenyatta University,* 2018.

[11] R. Hassan and B. Abubakar, "Intelligent arduino based automatic solar tracking system using light dependent resistors (LDRs) and servo motor," *Optics,* vol. 9, no. 2, p. 13, 2020, doi: 10.11648/j.optics.20200902.11.

[12] R. Saidur, S. Mekhilef, M. B. Ali, A. Safari, and H. A. Mohammed, "Applications of variable speed drive (VSD) in electrical motors energy savings," *Renewable and sustainable energy reviews,* vol. 16, no. 1, pp. 543-550, 2012, doi: https://doi.org/10.1016/j.rser.2011.08.020.

[13] F. Xie, C. Qiu, and Z. Qian, "Optimal speed–torque control of asynchronous motor for electric cars in the field-weakening region based on voltage vector optimization," *IEEE Transactions on Power Electronics,* vol. 37, no. 1, pp. 830-842, 2021, doi: 10.1109/TPEL.2021.3097906.

[14] W. Cai, X. Wu, M. Zhou, Y. Liang, and Y. Wang, "Review and development of electric motor systems and electric powertrains for new energy vehicles," *Automotive Innovation,* vol. 4, pp. 3-22, 2021, doi: https://doi.org/10.1007/s42154-021-00139-z.

[15] I. Cataldo, "Electric Vehicle for Mobility of Disabled People in Indoor Public Environment," 2022, doi: https://doi.org/10.46254/EU05.20220275.

[16] A. D. Kroemer and K. H. E. Kroemer, *Office ergonomics: Ease and efficiency at work*. CRC Press, 2016.

[17] M. Dooner, "Modelling, real-time simulation and control of automotive windscreen wiper systems for electronic control unit development," 2016.

JOURNAL OF AUTOMOTIVE AND MECHANICAL APPLIED TECHNOLOGY

Vol. 2 No. 1, 2025, pp. 93-101 https://journal.uny.ac.id/publications/jamat https://doi.org/10.21831/jamat.v2i1.1381

Design Analysis of Pancanaka 2000 Tooth Bucket Structure Using Finite Element Method

Raihan Fadhila[1], Yosef Budiman[2], Bambang Sulistyo[3*]

[1]Department of Mechanical and Automotive Engineering, Faculty of Vocational, Universitas Negeri Yogyakarta, 55652, Indonesia
[2]Automotive Engineering and Manufacturing Research Group, Faculty of Vocational, Universitas Negeri Yogyakarta, 55652, Indonesia
[3]Department of Automotive Engineering Education, Faculty of Engineering, Universitas Negeri Yogyakarta, 55281, Indonesia

*Corresponding author: bambang_sulistyo@uny.ac.id

ARTICLE INFO

Article history:
Received 16.03.2025
Revised 07.04.2025
Accepted 30.04.2025

Keywords:
Tooth bucket; Finite element analysis; Excavator; Cracking area

ABSTRACT

This study tests the structural performance of the Pancanaka 2000 tooth bucket, a common heavy-duty excavation component. The goals are to determine the component testing method, analyze the findings of finite element simulation sub-modeling, and identify the causes of structural failure. Shining 3D scanning created a detailed model of the Pancanaka 2000 tooth bucket. ANSYS simulation software performed a Finite Element Analysis on this model. A 10-ton static force was applied to imitate working circumstances on the bucket teeth tip. The simulation monitored mechanical reactions, including total displacement, von Mises stress, and safety factors, which indicate structural reliability. The study found numerous noteworthy findings. First, the computerized model of the bucket teeth allowed for an exact analysis of loading stress. The simulation revealed a region susceptible to failure under high loads, characterized by a maximum total displacement of 0.38883 mm, a maximum von Mises stress of 321.5 MPa, and a minimum safety factor of 1.328. Qualitative analysis identified material as the leading cause of fracture. Wear and scraping were noticed at the bucket tooth-adapter interface. Mechanical failure was also linked to component gaps exceeding design tolerance. These flaws lead to inappropriate load distribution and stress concentration, resulting in structural failure during operation. According to this study, the durability and performance of excavator components, such as the Pancanaka 2000 teeth bucket, depend on correct design, strict material selection, and precise assembly tolerances.

1. Introduction

Infrastructure development benefits various sectors, including economic, educational, social, cultural, agricultural, and others [1]. Developing countries like Indonesia continually undertake development initiatives in various sectors across the country. The number of development projects, both government and private, continues to grow over time. Apart from human resources, this development requires heavy equipment to provide support [2]. Technically, heavy equipment resources are the central element in implementing road projects. Heavy equipment is necessary to carry out road construction work efficiently and to meet predetermined goals. Heavy equipment (excavators) advantages include fast time, large power, and economic value. Heavy equipment (excavators) is a vital tool in the current era of development [3]. Therefore, special care is necessary to maintain the appearance of these devices. However, in some cases, the equipment is damaged.

Heavy equipment production continues to grow in Indonesia to meet the needs of consumers across various sectors, including agriculture, forestry, construction, and mining. According to data (Industrial Confidence Index January 2023 Increases Sharply, Industry Optimistic of Higher Growth in 2023) published by the Ministry of Industry of the Republic of Industry. The most significant increase in sales from January to August 2021 occurred in heavy equipment for the mining sector, which rose to 206% to 3,062 units from 1,001 units in the same period in 2020 [4]. The forestry sector increased by 84% to 1,487 units, the construction sector increased by 64% to 3,449 units, and the agro sector by 54.7% to 823 units. Heavy equipment production is estimated to reach 6,000 units by the end of 2021, representing a 75% increase from 2020, when around 3,427 units were produced [5]. Excavators are heavy equipment widely used to dig holes and make foundations in construction, mining, agriculture, and waste management [6]. Excavators have three primary structural components: the upper structure, the front attachment, and the undercarriage. One of the main components of the front attachment is the boom, arm, and bucket [7]. Front attachments have a significant role in executing tasks performed by excavators. An operator needs to understand the proper method of operating an excavator so that the tool is not vulnerable to damage [8].

The tooth bucket is one of the most important parts of the excavator bucket. Bucket teeth are useful as hard-breaking materials that function to avoid wear and damage to the bucket [7]. Bucket tooth damage due to wear will reduce the effectiveness of excavator work. Replacement of worn bucket teeth leads to high excavator operating costs. PT BISA Ruang Nuswantara is a social enterprise company that bridges and aligns education with the industrial sector to create opportunities for access to quality jobs. The company was officially established in April 2023 and is based on Delta Dunia Group's commitment to Environmental, Social, and Governance (ESG) aspects. In the same month, PT BISA Ruang Nuswantara separated from BUMA and operated as an independent entity, with a strong foundation in the Environmental, Social, and Governance (ESG) principles upheld by the Delta Dunia Group. PT BISA Ruang Nuswantara continues to play a crucial role in the group and is ambitious to expand its scope beyond the mining sector, exploring other sectors, including hospitality, to support government programs [9].

PT BISA Ruang Nuswantara is committed to empowering communities and ensuring a sustainable future through vocational education, innovation in the circular economy, and community empowerment initiatives. By leveraging its resources, expertise, and partner network, BIRU seeks to create value for all stakeholders while addressing some of Indonesia's most pressing social and environmental challenges today [9]. Through its vocational education program, PT BISA Ruang Nuswantara is dedicated to equipping young people with the essential skills, knowledge, and certifications necessary to succeed in the rapidly evolving job market. In addition, PT. BISA Ruang Nuswantara collaborates with universities in the country to design, manufacture, and distribute waste recycling products based on proven research. Through community empowerment initiatives, BIRU also supports micro, small, and medium enterprises (MSMEs) in creating new economic opportunities for communities and ensuring the sustainability of these enterprises [9]. PT BISA Ruang Nuswantara implements circular economy principles in industrial waste management to reduce environmental impact and support sustainability. By recycling low-carbon steel waste into value-added products such as tooth buckets and Allugoro hammers that meet high safety standards, PT BISA Ruang Nuswantara successfully reuses previously considered waste. In addition, the innovation of Eco-on Engineering Tools, which improves fuel efficiency, reflects BIRU's commitment to optimizing resource use, reducing carbon emissions, and creating a greener and more sustainable future for the industrial sector [9].

The problems I encountered with the Pancanaka 2000 tooth bucket involved several important technical aspects, including damage to the bottom of the tooth bucket, unstable conditions during installation, and repeated fractures over a relatively short period (by hour meter) can be show in Fig. 1. In addition, erosion resulted in a rounded tooth shape and made it difficult to penetrate the material, especially when 70% of the tooth length remained. These issues indicate design or material deficiencies that impact the durability and performance of the bucket teeth in difficult operational situations [10].

Figure 1. The tooth bucket bottom was broken

The cause of damage to the tooth bucket can be identified through several technical factors. One of them is excessive endplay dimensions, which result in uncontrolled movement and instability during operation. The design of tooth side angles that are too sharp can also accelerate the wear process and cause damage to the structure [11]. Additionally, undetected laminations can reduce the material's strength, thereby increasing the likelihood of fracture [12]. The high hardness of the material makes the tooth more susceptible to cracks. At the same time, worn adapters contribute to malfunction, as they reduce the effectiveness and stability of the tooth's joining under severe working conditions.

This research is necessary to investigate the causes of Pancanaka 2000 bucket tooth damage by employing a simulation approach through submodeling and interviews. Sub-modeling simulation examines in detail the stress distribution and mechanical factors that contribute to the occurrence of damage. At the same time, interviews are conducted to collect information directly from relevant parties regarding operational conditions, materials used, and other possible causes. Combining these two methods aims to gain a more comprehensive understanding, enabling the implementation of appropriate solutions to prevent similar damage from recurring in the future.

2. Methodology

This research employs evaluation and testing methods to investigate the causes of cracks in the Pancanaka 2000 tooth bucket, focusing on structural analysis using Ansys software simulation. If the simulation results did not provide a solution, the research continued with validation through interviews with the supervisor and staff regarding the common causes of tooth bucket fractures, based on 2021 company data. Additional references from interviews or field studies were also conducted, where possible, to confirm the veracity of the problem based on the chronology and on-site facts. This research refers to the following approach: 1) Primary observation, which involves examining the company's 2021 data regarding the physical condition of the Pancanaka 2000 tooth bucket, and 2) 3D scanning, which is done by scanning real objects to undergo a simulation testing process using software, and 3) Consists of pre, process, and evaluation stages.

Researchers reviewed various literature sources to identify existing problems and collect research data. The data used in this research includes types of evaluations and testers obtained from literature sources such as relevant journals, books, and articles. The data collection process is carried out by referring to the Pancanaka tooth bucket damage data in 2021 and collecting coherent information according to the research topic. Writing in the literature study stage involves incorporating quotes of facts from the field that aim to support this research.

The researcher scans the object under test using Shining 3D and dimensional instruments, adjusting them based on geometry and details to accurately and realistically replicate the toothed bucket the company has cast. This process aims to develop a model that can be applied in load analysis according to the specific needs in the field. The data obtained from the scan is then applied in 3D modeling using Ansys software. Ansys software is used to simulate static structural testing carried out by researchers.

Meshing breaks a continuous structural model into smaller components [13]. Better meshing quality, indicated by a larger number of elements the software can read, will result in higher convergence rates, reflecting better analysis accuracy. Given the complexity of the geometry required in tooth bucket modeling, it is crucial to determine suitable meshing techniques and methods at this stage so that the number of elements and nodes in the tooth bucket model can be evenly distributed efficiently. The simulation process is the stage that presents the analysis results based on the boundary conditions and loads determined during the Simulation Pre-Processing stage. In general, the results of this analysis display load contours marked with colors that reflect annotated values and directions, as well as specific information presented in both tabular and graphical form. Simulation processing is performed by analyzing the area at risk of cracking. Several loading result parameters appear until the discretization process is complete, focusing on three (3) main parameters.

Furthermore, the data summary stage aims to obtain a comprehensive summary of simulation testing results based on three key parameters. The data summary is presented as tables and graphs illustrating the simulation results. With this data summary, the author can conduct a more informed discussion in theoretical data analysis. In a theoretical context, the data analysis presents results and discussions that include the relationship between the findings obtained from the simulation and the relevant theories in this study. The data analysis process aims to extract useful information from data, which can be used to inform decisions and solve problems. The results of the data analysis will be presented in the form of conclusions that summarize the results obtained by researchers, both qualitatively and quantitatively, in the subsequent discussion of the simulation results.

The research conducted by the researcher lasted for 5 months, from February 16 to June 30, 2024. This research was conducted at the Research and Development department in the Engineering Department of PT BISA Ruang Nuswantara (BIRU), located at South Quarter Tower A, Penthouse Floor, Jalan R.A. Kartini Kav. 8, West Cilandak, Jakarta 12430. Research variables in the study "Design Analysis of Pancanaka 2000 Tooth Bucket Structure Using Finite Element Analysis Method" include independent variables, namely Ansys software as a loading simulation tool; dependent variables, namely the loading conditions of the analyzed Pancanaka 2000 tooth bucket; and controlled variables, namely factors that affect the results of computer testing, which require recalculation in case of errors or invalid data. An analytical model is a systematic approach to designing, conducting, and evaluating a study. Various research methods can be employed, and the selection of a method is determined by the research question, the objectives to be achieved, and the type of data required to address the problem under study.

3. Result and Discussion

Through the Shining 3D software, the original shape of the tooth bucket can be identified. A three-dimensional representation can be generated and converted into the format to be applied in this study, as shown in Fig. 2. Three-dimensional data of the Pancanaka 2000 tooth bucket was collected using the Shining 3D software, which scans a physical object to generate a highly detailed 3D model with X, Y, and Z coordinate axes in the desired direction. Despite being relatively new, this 3D scanning technology is considered accurate, fast, and effective. The scanning procedure was conducted according to SOPs to ensure data accuracy and consistency. The resulting 3D model serves as the basis for the testing and simulation stage, utilizing Ansys software to analyze product performance through simulations of material strength, load resistance, and environmental impact. These simulations aim to ensure the product meets quality standards and provide insights for further development.

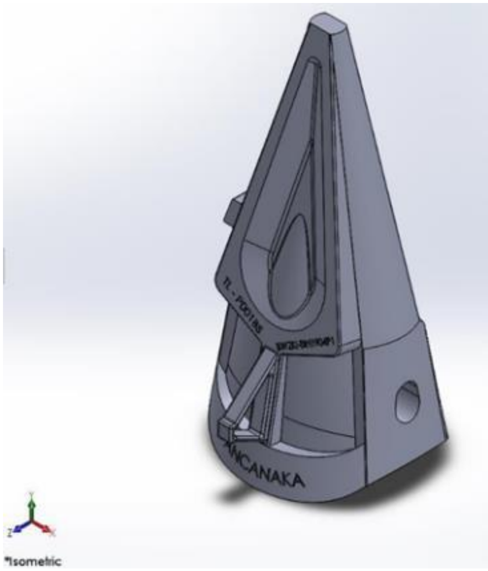

Figure 2. 3D scan results have been converted

Three-dimensional data of the Pancanaka 2000 tooth bucket were collected using Shining 3D software, which scans physical objects to produce highly detailed 3D models in the desired direction along the X, Y, and Z coordinate axes. Despite being relatively new, this 3D scanning technology is considered accurate, fast, and effective. The scanning procedure was conducted according to SOPs to ensure data accuracy and consistency. The resulting 3D model serves as the basis for the testing and simulation stage, utilizing Ansys software to analyze product performance through simulations of material strength, load resistance, and environmental impact. These simulations aim to ensure the product meets quality standards and provide insights for further development. The approach applied in testing the tooth bucket structure is through simulation modeling. This method analyzes the cracking area as part of the test. The cracking area analysis stage displays the overall simulation conditions, including the bucket used at the site, which has a capacity of 13.7 m^3, allowing for a material lift of 20 tons per lift. When digging 10 tons, the converted load is 98,066 N.

A thorough analysis was conducted to identify the part of the bucket tooth that experienced the heaviest loading, which was marked with a red contour for further analysis. A simulation of the cracking area was conducted, considering three analysis parameters, to validate the tooth bucket's ability to withstand the load. Assuming a similar fixed support position. Total deformation reflects the state of loading that causes dislocation or deformation before reaching the yield strength point. In this context, the deformation occurs in an elastic state, allowing it to return to its original position. This aspect is important because it affects the safety and durability of materials used in construction. The higher the applied test stress, the greater the displacement, which in turn results in decreased safety.

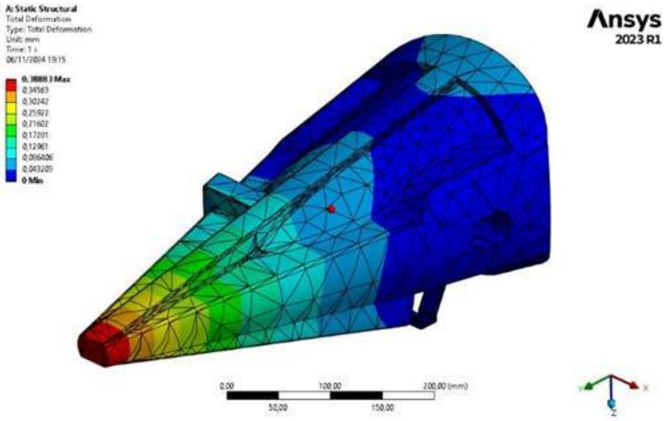

Figure 3. Total deformation results

Based on Fig. 3, it can be seen that the red contour shows a high deformation rate of 0.38883 mm. This value reflects a minimal deformation of less than 1 mm, which allows the tooth bucket to return to its original position. Meanwhile, the lowest deformation value was recorded at 0 mm at the back of the bucket tooth, indicating that the area was not subjected to significant stress. In von Mises stress, there is a relationship between the loading conditions and the stress distribution in the material, so a simulation is performed to illustrate the value of von Mises stress. The von misses stress is an indicator to assess the possibility of material failure by analyzing the results of the three main stresses, which are often referred to as principal stresses. Material failure can be predicted when the von Mises stress value exceeds the yield stress of the material (σv> σy).

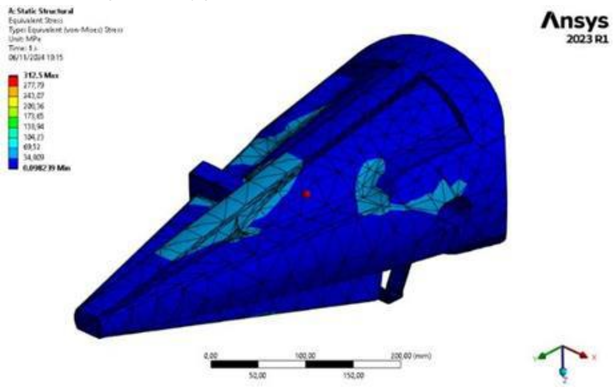

Figure 4. Von misses the stress results

In Fig. 4, the von misses stress analysis shows that the largest stress occurs inside the bucket tooth, which functions to withstand the load during the excavation process. The maximum measured stress value reached 312.5 MPa. Meanwhile, the low-stress value is 0.0982 MPa. An important parameter that supports static structural analysis is the safety factor. The safety factor plays a crucial role in ensuring that the system remains safe when facing loads exceeding calculations, so the design does not fail under these conditions. A higher safety factor value indicates that the construction has a better and stronger ability to withstand loads. In this study, the minimum safety factor is set at 1.5, which is considered based on material safety aspects.

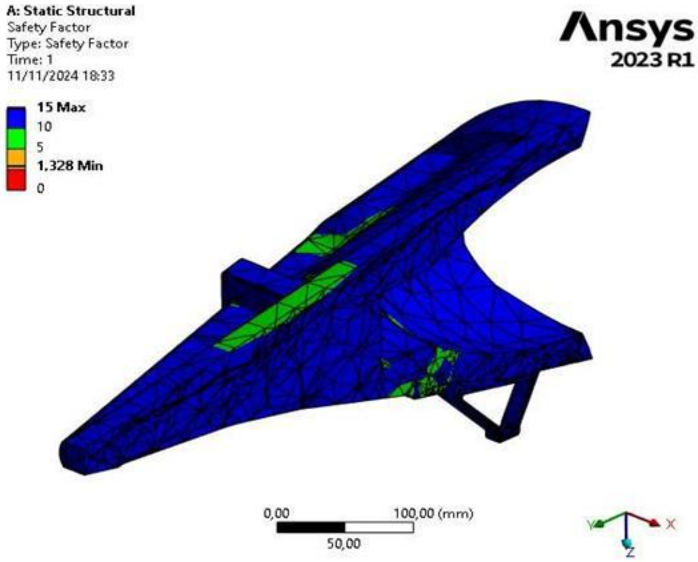

Figure 5. Safety factor analysis results

Fig. 5 shows that the highest safety factor value reaches 15 in the control zone area and its surroundings, which are marked in several annotated sections. Meanwhile, the low safety factor value is 1.328 in the safety zone. Although some elements fall below the minimum standard, this does not affect the existing loads. The analysis results show that von misses stress occurs inside the bucket tooth, which functions to withstand the load during the excavation process. The maximum measured stress value reached 312.5 MPa, while the lowest was only 0.0982 MPa. According to the data, the maximum stress that occurs is still below the characteristic yield strength of AISI 4140 material, which is 655 MPa. This shows that the material can withstand the workload. However, areas with high stress still require special attention to prevent potential damage in the future [14].

The results of the total displacement analysis show that the largest deformation occurs at the tip of the bucket tooth, where this elastic condition allows the material to return to its original position after the load is released. The maximum deformation value measured reached 0.38883 mm. In comparison, the lowest deformation value was 0 mm, indicating a variable load distribution on the component. This indicates that the tip of the tooth bucket is the most vulnerable area to deformation due to the working load. However, the deformation that occurs remains within reasonable limits for the material used, consistent with its elasticity characteristics. Sun, Yuan, et al. [15] stated that the tip of the tooth bucket often experiences the highest deformation when it receives the maximum working load under digging conditions. The safety factor indicates that the construction has a better and stronger ability to withstand loads, ensuring the structure can withstand extreme conditions. The maximum safety factor value measured reached 15, indicating that the structural design is significantly stronger than the facing load. Meanwhile, the low safety factor value of 1.328 indicates that the minimum safety factor result is still below the set 1.5, considering material safety aspects [13, 16].

4. Conclusion

Based on the results of the research and discussion that have been carried out regarding the Design Analysis of the Pancanaka 2000 Tooth Bucket Structure using the Finite Element Analysis Method, several conclusions can be drawn as follows:

1) The analysis was carried out with parameters, including total displacement, von Mises stress, and safety factor, through simulation using Ansys software. A load of 10 tons was applied, corresponding to a loading of 98066 N, which was distributed to the part where cracking was found.
2) Simulated test results show Total Displacement: 0.38883 mm, Von Mises-Stress: 312.5 MPa, and Safety Factor: 1,328. The company's product is structural steel material. The current loading condition allows the Pancanaka 2000 tooth bucket to return to its original state by maintaining its shape.
3) Factors that cause the Pancanaka 2000 tooth bucket to break include material erosion of the tooth adapter, resulting in the tooth bucket gap exceeding the tolerance limit (0.5 mm to 1.5 mm), and environmental factors that affect operational units in two areas: rocky and sandy. In rocky conditions, the tooth bucket often breaks on its back. The tooth bucket is corroded in sandy conditions, or the tip is blunted quickly.

Conflict of interest

The authors declare that they have no conflict of interest.

References

[1] J. Joeliaty, "The Impact of Infrastructure Development, Education, Tourism, and Agriculture on Regional Economic Growth in Indonesia," *The Es Economics and Entrepreneurship,* vol. 2, no. 03, pp. 193-207, 2024, doi: https://doi.org/10.58812/esee.v2i03.235.

[2] A. Palomino-Valles, M. Tokumori-Wong, P. Castro-Rangel, C. Raymundo-Ibañez, and F. Dominguez, "TPM maintenance management model focused on reliability that enables the increase of the availability of heavy equipment in the construction sector," 2020 2020, vol. 796: IOP Publishing, 1 ed., p. 012008, doi: 10.1088/1757-899X/796/1/012008.

[3] A. U. Khan, L. Huang, E. Onstein, and Y. Liu, "Overview of emerging technologies for improving the performance of heavy-duty construction machines," *Ieee Access,* vol. 10, pp. 103315-103336, 2022, doi: 10.1109/ACCESS.2022.3209818.

[4] J. Verhoef, "The rise of chronic reachability and the accelerated, flexible society: The social construction of the pager, 1987–1999," *Mobile Media & Communication,* vol. 12, no. 3, pp. 617-636, 2024, doi: https://doi.org/10.1177/20501579231219353.

[5] D. S. Pradhan, A. K. Patra, S. Santra, A. Penchala, S. P. Sahu, and Nazneen, "In-cabin particulate matter exposure of heavy earth moving machinery operators in Indian opencast coal mine," *Aerosol Science and Engineering,* pp. 1-18, 2024, doi: https://doi.org/10.1007/s41810-024-00258-0.

[6] B. A. M. Mohan, M. U. Rahaman, R. Madhu, and M. B. Khot, "Finite element analysis & topology optimization of excavator bucket teeth for optimal performance," *Mining Technology,* vol. 133, no. 3, pp. 214-225, 2024, doi: https://doi.org/10.1177/25726668241270488.

[7] D. Sun *et al.*, "Analysis of the position recognition of the bucket tip according to the motion measurement method of excavator boom, stick and bucket," *Sensors,* vol. 20, no. 10, p. 2881, 2020, doi: https://doi.org/10.3390/s20102881.

[8] W. A. Tanoli, A. Sharafat, J. Park, and J. W. Seo, "Damage Prevention for underground utilities using machine guidance," *Automation in Construction,* vol. 107, p. 102893, 2019, doi: https://doi.org/10.1016/j.autcon.2019.102893.

[9] Deltadunia. "Company Profile BIRU. Delta Dunia Group." https://deltadunia.com/biru (accessed.

[10] Z. Dong, F. Jiang, Y. Tan, F. Wang, R. Ma, and J. Liu, "Review of the modeling methods of bucket tooth wear for construction machinery," *Lubricants,* vol. 11, no. 6, p. 253, 2023, doi: https://doi.org/10.3390/lubricants11060253.

[11] W. Zhai *et al.*, "Recent progress on wear-resistant materials: designs, properties, and applications," *Advanced Science,* vol. 8, no. 11, p. 2003739, 2021, doi: https://doi.org/10.1002/advs.202003739.

[12] V. Dikshit, S. K. Bhudolia, and S. C. Joshi, "Multiscale polymer composites: A review of the interlaminar fracture toughness improvement," *Fibers,* vol. 5, no. 4, p. 38, 2017, doi: https://doi.org/10.3390/fib5040038.

[13] A. Widyianto, A. S. Baskoro, and G. Kiswanto, "Design and Analysis of Orbital Pipe Welding Prototype for Piping System Welding Applications," *Journal of Automotive and Mechanical Applied Technology,* vol. 1, no. 1, pp. 11-23, 2024.

[14] S. J. Warden, W. B. Edwards, and R. W. Willy, "Preventing bone stress injuries in runners with optimal workload," *Current osteoporosis reports,* vol. 19, no. 3, pp. 298-307, 2021, doi: 10.1007/s11914-021-00666-y.

[15] Y. Sun *et al.*, "Digging Performance and Stress Characteristic of the Excavator Bucket," *Applied Sciences,* vol. 13, no. 20, p. 11507, 2023, doi: https://doi.org/10.3390/app132011507.

[16] T. Poutanen, T. Länsivaara, S. Pursiainen, J. Mäkinen, and O. Asp, "Calculation of safety factors of the Eurocodes," *Applied Sciences,* vol. 11, no. 1, p. 208, 2020, doi: https://doi.org/10.3390/app11010208.

JOURNAL OF AUTOMOTIVE AND MECHANICAL APPLIED TECHNOLOGY

Vol. 2 No. 1, 2025, pp. 102-110 https://journal.uny.ac.id/publications/jamat https://doi.org/10.21831/jamat.v2i1.1343

Development of an LDR-Integrated PDLC Film for Automatic Glare Reduction in Vehicles

Riyan Ikhsan Nugroho[1], Marcin Noga[2], Naufal Annas Fauzi[1*]

[1]Department of Mechanical and Automotive Engineering, Faculty of Vocational, Universitas Negeri Yogyakarta, Kulon Progo, Yogyakarta 55652, Indonesia
[2]Faculty of Mechanical Engineering, Cracow University of Technology 31-155, Poland

*Corresponding author: naufalannasfauzi@uny.ac.id

ARTICLE INFO

Article history:
Received 02.04.2025
Revised 30.04.2025
Accepted 14.05.2025

Keywords:
PDLC Film; Glare Reduction; Light Dependent Resistor; Smart Tinting System; Vehicle Safety

ABSTRACT

The high risk of glare from vehicle headlights at night often becomes a significant contributor to traffic accidents, particularly for motorcyclists and drivers of lightweight vehicles. To address this issue, a smart glare-blocking system based on a PDLC (Polymer Dispersed Liquid Crystal) film has been developed. This research proposes the design, development, and testing of a PDLC film system integrated with an LDR (Light-Dependent Resistor) sensor to automatically detect light intensity and adjust the film's opacity in real-time. The goal is to enhance driver visibility and comfort without compromising overall road safety. The experimental setup involved placing the prototype system at varying distances (0–9 meters) from a controlled light source at night. Measurements were conducted to collect data on light intensity, voltage output, resistance of the LDR, and the degree of light attenuation achieved by the PDLC film. The results showed that at a distance of 1 meter, the PDLC film could block up to 99.85% of incoming light, reducing 12080 Lux to only 17 Lux. Moreover, the film began to react at 6 meters with an output voltage of 34V. It became fully transparent at 8–9 meters with an output of 50V. The findings demonstrate that the PDLC system functions effectively in detecting potential glare and reducing its impact before it reaches the driver's eyes. This intelligent system offers a promising solution for minimizing night-driving hazards by dynamically adapting to changing light conditions.

1. Introduction

The headlamp, commonly referred to as the front light of a motor vehicle, plays a crucial role in ensuring driving safety, particularly during nighttime or adverse weather conditions [1, 2]. With the continuous advancement of technology in motor vehicles, headlamp technology has undergone significant evolution. However, this development has led to a recurring issue: glare. For decades, glare from oncoming vehicles has been a significant concern for drivers and traffic safety researchers globally. A 2019 study conducted in the United Kingdom revealed that approximately 60% of 1,215 drivers reported being dazzled by headlights from oncoming traffic, often struggling to distinguish between low-beam and high-beam lights. SUVs were often cited as frequent offenders due to their elevated lamp positions [3].

Nighttime driving is significantly riskier than daytime driving. According to Ackaah, W. et. al [4], the likelihood of vehicular accidents at night is three times higher than during the day, despite lower traffic volumes. Supporting this, the World Health Organization [3] reports around 1.3 million deaths annually due to road traffic accidents. In Indonesia, data from DataIndonesia.com indicate an increase in accident cases, rising from 100,028 in 2020 to 103,645 in 2021 [5]. One fatal incident in 2022 involved a motorcyclist who fell into a five-meter-deep construction hole after being blinded by high-beam lights from an oncoming vehicle [6].

National regulations, such as Indonesian Law No. 22 of 2009 and Government Regulation No. 55 of 2012, explicitly mandate that every motor vehicle must meet technical requirements and roadworthiness standards, including the lighting system. The misuse of headlamps that causes glare is thus a legal and safety concern. In another incident in 2022, a traffic accident involving three motorcycles and a car on the Daan Mogot flyover occurred due to glare from direct sunlight [7]. This highlights not only artificial but also natural sources of glare. Anjar Rosjadi, Head of Marketing Product Planning Division at Astra Daihatsu Motor, emphasized that sun visors are explicitly designed to minimize such sun glare [8].

Sun visors are standard equipment in almost all vehicles, designed to reduce direct sunlight and enhance driver comfort. However, as noted by Tutunea, D. et al. [9], the design of sun visors has remained relatively unchanged since the 1930s. Given this stagnation, alternative solutions are necessary to enhance visual comfort and driving safety. One promising alternative is the use of Polymer Dispersed Liquid Crystal (PDLC) film, which consists of a thin polymer layer embedded with liquid crystal (LC) microdroplets dispersed within a matrix. PDLC films can change from opaque to transparent states when an applied voltage is applied, making them a suitable substitute for conventional sun visors [10, 11]. However, a major limitation lies in the control unit, which is often costly, with commercial controllers priced over six million Indonesian Rupiah, as observed in online markets.

Integrating PDLC film into automotive sun visor systems offers the potential for dynamic, electronically controlled glare reduction. However, a research gap remains in developing cost-effective control mechanisms and evaluating their effectiveness in real-world driving conditions. Prior studies have highlighted the importance of adaptive systems in reducing glare and improving visibility [12]. Therefore, this study aims to explore the feasibility of a smart PDLC-based anti-glare system as an innovative and affordable alternative to conventional sun visors.

2. Methodology

2.1 Research Design

The experimental testing was conducted to assess the performance of a PDLC (Polymer Dispersed Liquid Crystal) film system in automatically adjusting its transparency in response to varying levels of light intensity. The test aimed to simulate real-world lighting conditions particularly exposure to motorcycle headlamps under controlled nighttime conditions, eliminating ambient light interference as recommended in similar smart window evaluations [13].

The core components of the system included a motorcycle headlamp as the primary light source, a transparent acrylic sheet embedded with PDLC film, an LDR (Light Dependent Resistor) sensor for light detection, a control circuit for voltage regulation, a digital lux meter to measure light intensity, and a digital multimeter to monitor the resistance and output voltage. The PDLC film, in this system, would adjust its opacity based on the electrical signal derived from the LDR's response to incoming light, similar to approaches used in automotive glare-reduction systems [14].

To facilitate the measurements, a measuring tape was extended in a straight line from the headlamp, marking distances from 0 to 9 meters. At each distance point, the PDLC film module, including the LDR sensor and control circuitry, was positioned. The lux meter was initially used to record the light intensity before the light passed through the PDLC film. Following this, the multimeter recorded the resistance of the LDR, and the output voltage from the control circuit was measured. Finally, the lux meter was placed behind the PDLC panel to measure the amount of light that passed through the film, thereby evaluating the film's ability to block or transmit light.

Measurements were taken sequentially at each one-meter interval, starting from 0 meters up to 9 meters. This process allowed for the observation of how the system responded to decreasing light intensity as the distance increased. To ensure data accuracy and minimize anomalies, the voltage output test was repeated thirty times under the same conditions. The data collected from these repeated tests were compiled into a voltage response curve to visualize consistency and system behavior, in line with experimental validation standards for optical smart materials [15].

The observations were carefully documented in a series of tables that showed the relationship between distance and various parameters, including incoming lux values, LDR resistance, output voltage, and the percentage of light blocked by the PDLC film. These results were then analyzed further through graphical representations, illustrating how the PDLC film system adapted to light intensity by modulating its transparency in real-time.

This experimental procedure successfully demonstrated the system's effectiveness in dynamically responding to varying light inputs. The PDLC film was proven to block significant amounts of light under high-intensity exposure and allow greater transmittance under dimmer conditions, verifying the functional integration between the sensor, control circuit, and PDLC technology.

2.2 Experimental Instrument

The accuracy and reliability of the instruments used in the study are crucial for obtaining valid results. All instruments used in this study were verified to meet the proper technical standards and were calibrated prior to data collection. The digital lux meter and multimeter used had sufficient resolution and accuracy to ensure reliable measurements in a laboratory setting. The instruments used in this study are summarized in Table 1:

Table 1. The instruments used in this study

No	Instrument	Specification
1	Digital Lux Meter	Measurement range: 0–200,000 lux; Accuracy: ±4% + 10; Resolution: 1 lux
2	Digital Multimeter	- DC Current: up to 10A; Accuracy: ±1.0% + 5 digits; Resolution: 0.01A - DC Voltage: up to 600V; Accuracy: ±0.5% + 3 digits; Resolution: 0.001–0.1V - Resistance: up to 60MΩ; Accuracy: ±0.8% + 3 digits; Resolution: 0.1Ω–0.01MΩ
3	Measuring Tape	Used to measure light source distance precisely
4	Stationery Tools	For manual recording of measurements during the experiment

2.3 Instrument Validation and Data Analysis

The collected data were analysed using descriptive statistics. For each variable (light intensity, sensor resistance, and output voltage), the mean, minimum, and maximum values were calculated to examine the overall response of the system. In addition, percentage changes in voltage were used to assess the level of transparency as the light intensity varied with distance. The analysis applied the following basic formulas, as shown in Eqs. 1 and 2.

$$\bar{x} = \frac{\sum x}{n} \tag{1}$$

Where : $\bar{x}$ = Mean

x = Observed Value

n = Number of observations

$$P = \frac{\sum x}{Total\ value} \times 100\% \quad (2)$$

Where : P = Percentage
x = Observed Value

3. Result and Discussion

3.1 Prototype

The PDLC film device prototype was designed and developed with a focus on controlling the voltage output through an LDR (Light Dependent Resistor) sensor, which operates based on the principle of a voltage divider. In this research, the LDR's resistance is used to read light conditions, as the resistance of the LDR changes with varying light intensity. The LM317HV integrated circuit (IC) was chosen to regulate the output voltage based on the resistance of the LDR. As the distance between the light source and the LDR sensor increases, the resistance of the LDR decreases, causing the LM317HV to output higher voltage levels, which in turn control the PDLC film. The voltage output curve, generated from the experimental results, is shown in Figure 4.11. Polynomial regression analysis was used to model the relationship between light intensity and the output voltage.

The system operates with an AC power supply (PLN), which is converted to 12V DC through a PSU (Power Supply Unit) with a 10A capacity. The 12V DC is then routed through a main switch to control the device's power. This voltage is subsequently distributed to a cooling fan, a DC-to-DC step-down converter, and a DC-to-DC step-up converter. The step-down converter reduces the voltage from 12V to 5V, supplying power to the Arduino board, DHT11 temperature sensor, and a 5V relay. Meanwhile, the step-up converter increases the voltage to 50V, which the PDLC controller then adjusts to manage the PDLC film. The system schematic is shown in Fig. 1, which illustrates the complete voltage distribution and flow throughout the device.

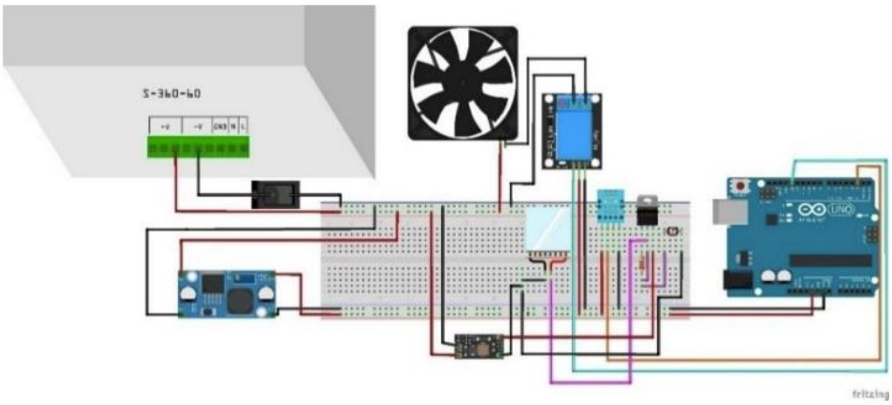

Figure 1. Schematic of the system

The PDLC controller circuit employs the LM317HVT IC to regulate the voltage supplied to the PDLC film. The LM317HVT IC has three pins: the adjust pin, the output pin (V_{out}), and the input pin (V_{in}). The adjust pin is connected to the LDR, which acts as the input sensor to monitor light intensity. The resistance from the LDR affects the output voltage when an input voltage of 57V is applied. The LM317HVT adjusts the output voltage accordingly, enabling the

PDLC film to react to varying light conditions [16]. The detailed schematic for the PDLC controller is shown in Fig. 2.

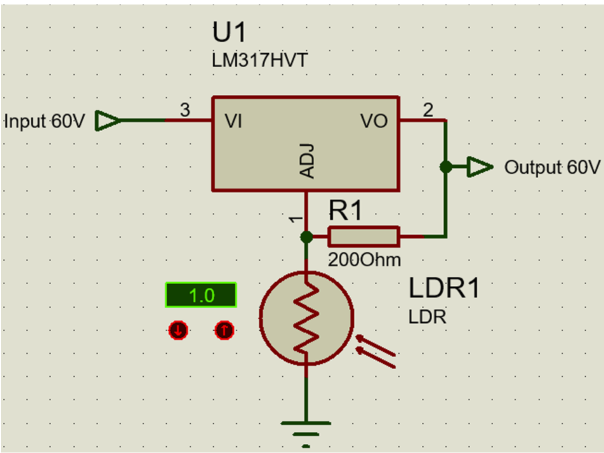

Figure 2. Schematic wiring diagram PDLC

A cooling system was implemented to maintain the temperature of the components within the normal operating range. The 12V power supply from the PSU powers the system, and this voltage is distributed to a cooling fan. A DC-to-DC converter is used to step down the voltage to 5V, which supplies power to the Arduino board, DHT11 sensor, and relay. The cooling system is controlled via software written in Arduino IDE, ensuring that the fan operates when needed to prevent overheating of the system during operation [17]. The complete assembly of the prototype is shown in Fig. 3.

Figure 3. Assembly of the prototype

3.2 Prototype Testing

As illustrated in Fig. 4, the output voltage of the PDLC film system increased linearly with the distance from the light source. At a distance of 1 meter, the system recorded an output voltage of 9.8 V, corresponding to a light intensity reading of 12,080 kilolux. This relationship suggests that the closer the distance to the light source, the higher the intensity measured by the sensor, and consequently, the greater the voltage output. As the distance increased, the voltage reached 50V at a distance of 8 meters, demonstrating that the PDLC film system becomes fully transparent, thereby ensuring better visibility for the driver [18].

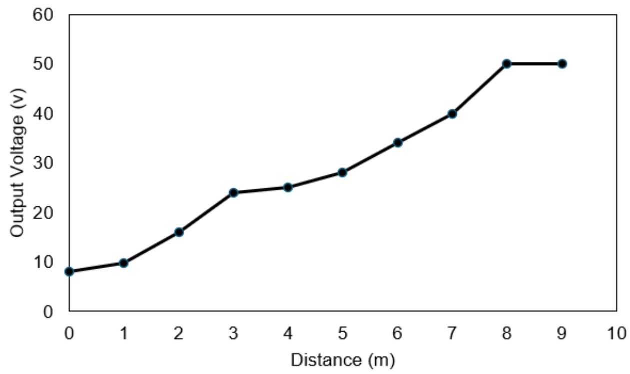

Figure 4. Measured Light Intensity and Corresponding Output Voltage Based on Distance from Light Source

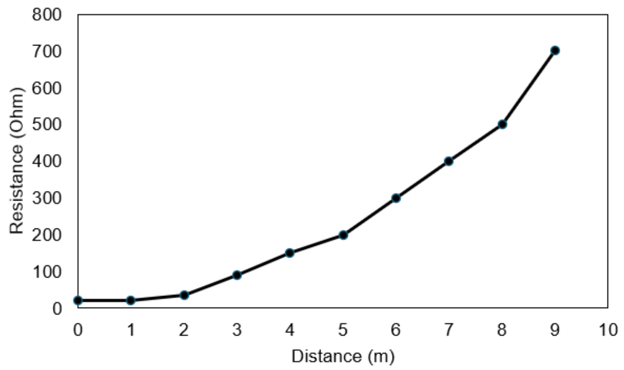

Figure 5. Table of Light Intensity and LDR Resistance at Various Distances from the Light Source

At 6 meters, the PDLC film began to function optimally, with a voltage of 34V and a light intensity of 277 lux. This result aligns with the system's goal of adjusting the opacity of the PDLC film in response to light intensity, thereby effectively protecting the driver from potentially blinding light [19]. The system's ability to block light gradually diminished as the distance increased, with the PDLC film becoming fully opaque at a distance of 2 meters, blocking 99.98% of the light, as shown in Table 2.

Table 2. Percentage Change in Lux Levels with Distance

No	Distance (m)	Lux Before	Lux After	Percentage (%)
1	0	158400	30	99.98
2	1	12080	17	99.85
3	2	2990	28	99.06
4	3	1300	40	96.92
5	4	623	56	91.01
6	5	425	53	87.52
7	6	277	41	85.11
8	7	162	30	81.48
9	8	111	23	79.27
10	9	83	45	45.78

Fig. 5 presents the resistance of the LDR and the corresponding voltage output for each distance and light intensity. The resistance of the LDR decreased with increasing light intensity, which is expected due to the nature of LDRs [20]. As the light intensity increases, the resistance of the LDR decreases, allowing more current to pass through, thereby increasing the output voltage. This trend is evident from the measurements, as the resistance at 1 meter was 20 Ohms. In contrast, at 9 meters, it rose to 700 Ohms, reflecting the decrease in light intensity with distance.

At a distance of 1 meter, the LDR measured a light intensity of 12,080 lux, resulting in a relatively low resistance of 20 Ohms. At this point, the PDLC film was able to block a significant amount of light (99.85%), reducing the lux value from 12,080 lux to 17 lux. This shows that the PDLC film is highly effective at close range, with a light-blocking efficiency of 99.85%, as indicated in Table 2. However, as the distance increased, the light-blocking efficiency gradually decreased. At 9 meters, the light-blocking efficiency dropped to 45.78%, where the lux value after passing through the PDLC film was recorded as 45 lux [21].

4. Conclusion

The testing of PDLC film technology, both experimental and analytical, led to important conclusions regarding its performance and suitability for use in automotive applications. The system effectively reacts to variations in light intensity. The transparency of PDLC film shifts dynamically when exposed to light, particularly from nearby sources such as headlights or bright sunlight. The movie becomes unclear when exposed to bright lights from a short distance. This feature minimizes glare and enhances visibility for drivers, particularly in situations where bright light may pose a safety risk.

The second conclusion highlights the system's output voltage. The output voltage increases linearly with the distance of the light source. At a distance of 1 meter, the voltage measures 9.8 volts, while at 8 meters, it increases to 50 volts. The voltage regulates the transparency of the PDLC film, creating a reliable connection between the light intensity, the resistance of the LDR sensor, and the system's output voltage. Predictability is essential for refining the film's behavior in real-world scenarios. The short-range light-blocking effectiveness of PDLC film is outstanding. The film blocks as much as 99.98% of light at a distance of 0 meters. It has an effectiveness of over 80% at distances of up to 7 meters, making it suitable for a wide range of practical uses. After 8 meters, efficiency starts to decline, reaching its lowest blocking capability of 45.78% at 9 meters. This drop indicates an optimal operational range where the system performs most effectively.

The activation range of the system is another significant outcome. The PDLC film reacts to light at a distance of 6 meters when provided with a 34-volt output voltage and a light intensity of 277 lux. The system becomes increasingly transparent from this point, achieving complete transparency at a distance of 8 meters. On the other hand, complete opacity at 2 meters enables the system to respond to varying lighting conditions and maintain driver visibility instantly. The experiments demonstrate that the PDLC film system is suitable for use in automotive settings. The adaptive light-filtering enhances both driver comfort and safety. This device minimizes glare from oncoming headlights and intense sunlight, enhancing safety and comfort while driving in low-visibility or high-glare situations. The results indicate that the PDLC film presents a dependable and innovative option for vehicle design.

Conflict of interest

The authors declare that they have no conflict of interest.

References

[1] P. Boyce, *Lighting for Driving: Roads, Vehicles, Signs, and Signals: Roads, Vehicles, Signs, and Signals*. CRC Press, 2024.

[2] G. Toney and C. Bhargava, "Adaptive headlamps in automobile: A review on the models, detection techniques, and mathematical models," *IEEE Access,* vol. 9, pp. 87462-87474, 2021, doi: 10.1109/ACCESS.2021.3088036.

[3] M. Harrison, *On the Road to Victory: The Rise of Motor Transport with the BEF on the Western Front*. Pen and Sword, 2020.

[4] W. Ackaah, B. A. Apuseyine, and F. K. Afukaar, "Road traffic crashes at night-time: characteristics and risk factors," *International journal of injury control and safety promotion,* vol. 27, no. 3, pp. 392-399, 2020, doi: 10.1080/17457300.2020.1785508.

[5] N. S. Kusumastutie, B. Patria, S. Kusrohmaniah, and T. D. Hastjarjo, "A review of accident data for traffic safety studies in Indonesia," 2024, vol. 1294: IOP Publishing, 1 ed., p. 012012, doi: 10.1088/1755-1315/1294/1/012012.

[6] C. Luo, G. Xin, H. Xu, and W. Tang, "Glare-free high-beam control for oncoming vehicle safety in nighttime," *IEEE Consumer Electronics Magazine,* vol. 10, no. 2, pp. 8-15, 2020, doi: 10.1109/MCE.2020.3040724.

[7] S. Banerjee, "A study on the effect of light in road accident prevention and promotion of pedestrian safety," 2019, doi: 10.24906/isc/2022/v36/i4/216417.

[8] V.-I. Ungureanu, R.-C. Miclea, A. Korodi, and I. Silea, "A novel approach against sun glare to enhance driver safety," *Applied Sciences,* vol. 10, no. 9, p. 3032, 2020, doi: https://doi.org/10.3390/app10093032.

[9] D. Tutunea, A. Dima, M. Bica, and M. Buculei, "The design of sun visors for automotive industry," *Annals of the University of Oradea. Fascile of Management and Technological Engineering,* pp. 124-127, 2014, doi: 10.15660/AUOFMTE.2014-3.3083.

[10] R. R. Deshmukh, "Electro-optic and dielectric responses in PDLC composite systems," *Liquid Crystalline Polymers: Volume 2--Processing and Applications,* pp. 169-195, 2015, doi: https://doi.org/10.1007/978-3-319-20270-9_7.

[11] S. D. Rezaei, S. Shannigrahi, and S. Ramakrishna, "A review of conventional, advanced, and smart glazing technologies and materials for improving indoor environment," *Solar Energy Materials and Solar Cells,* vol. 159, pp. 26-51, 2017, doi: https://doi.org/10.1016/j.solmat.2016.08.026.

[12] J. D. Bullough, N. P. Skinner, and T. T. Plummer, "Adaptive driving beam headlights: visibility, glare and measurement considerations," Rensselaer Polytechnic Institute. Lighting Research Center, 2016.

[13] N. Wang *et al.*, "Self-adaptive PDLC control strategy with smart light intensity adjustment using photovoltaic-thermoelectric hybrid energy supply technology," *IEEE Transactions on Industrial Electronics,* vol. 70, no. 10, pp. 10146-10155, 2022, doi: 10.1109/TIE.2022.3224166.

[14] J. Sumithra, A. Sumalatha, A. Vanitha, B. Sivadharshini, V. S. Pandi, and S. Ravi, "A Smart and Systematic Vehicle Headlight Operations Controlling System based on Light Dependent Resistor," 2024: IEEE, pp. 1-6, doi: 10.1109/IITCEE59897.2024.10467948.

[15] M. S. Islam *et al.*, "Performances of polymer-dispersed liquid crystal films for smart glass applications," *Polymers,* vol. 15, no. 16, p. 3420, 2023, doi: https://doi.org/10.3390/polym15163420.

[16] Z. Zhang *et al.*, "A novel low-voltage fast-response electrically controlled dimming film based on fluorinated PDLC for smart window applications," *Chemical Engineering Journal,* vol. 479, p. 147668, 2024, doi: https://doi.org/10.1016/j.cej.2023.147668.

[17] N. A. Junizan, A. A. Razak, B. Balakrishnan, and W. Othman, "Design and implementation of automatic room temperature controlled fan using Arduino Uno and LM35 heat sensor," *International Journal of Engineering Creativity & Innovation,* vol. 1, no. 2, pp. 8-14, 2019.

[18] W. Yin *et al.*, "A recyclable, interchangeable optical switch with a PDLC-PVA-PSCLC structure and a low-voltage drive system," *Liquid Crystals,* vol. 51, no. 11, pp. 1942-1955, 2024, doi: https://doi.org/10.1080/02678292.2024.2372603.

[19] H. Gundogdu, M. Terkes, A. Demirci, and U. Cali, "Assessing energy savings and visual comfort with PDLC-based smart window in an Istanbul office building: A case study," *Energy Reports,* vol. 12, pp. 4252-4265, 2024, doi: https://doi.org/10.1016/j.egyr.2024.10.009.

[20] W. Setya, A. Ramadhana, H. R. Putri, A. Santoso, A. Malik, and M. M. Chusni, "Design and development of measurement of measuring light resistance using Light Dependent Resistance (LDR) sensors," 2019, vol. 1402: IOP Publishing, 4 ed., p. 044102, doi: 10.1088/1742-6596/1402/4/044102.

[21] K. Kang and Y. Li, "Research on optical efficiency of heliostat field based on cosine loss model and shadow light blocking efficiency model," *International Journal of Frontiers in Engineering Technology,* vol. 5, no. 12, 2023.

JOURNAL OF AUTOMOTIVE AND MECHANICAL APPLIED TECHNOLOGY

Vol. 2 No. 1, 2025, pp. 111-123 https://journal.uny.ac.id/publications/jamat https://doi.org/10.21831/jamat.v2i1.1423

Development of Special Service Tools Tracker Kingpin Hino Series 300 to Increase Technician Work Efficiency

Adhe Satria Ramadhan[1], Yoga Guntur Sampurno[1*]

[1]Department of Mechanical and Automotive Engineering, Faculty of Vocational, Universitas Negeri Yogyakarta, Kulon Progo, Yogyakarta 55652, Indonesia

*Corresponding author: yoga_guntur@uny.ac.id

ARTICLE INFO

Article history:

Received	29.04.2025
Revised	18.05.2025
Accepted	04.06.2025

Keywords:

Tracker kingpin; Special service tools; Finite element analysis; Hino series

ABSTRACT

This study focused on the design, development, and evaluation of a Special Service Tool (SST) created explicitly for maintaining kingpin components in Hino Series 300 trucks. The research focused on the challenges and safety issues encountered by technicians stemming from the lack of specialized tools for kingpin removal. This often led to extended service times, variable repair quality, and a heightened risk of damaging components. To address these challenges, the research employed the ADDIE development model, which comprises five stages: Analysis, Design, Development, Implementation, and Evaluation. In the design phase, 3D modeling was performed using SolidWorks, and Finite Element Analysis (FEA) was conducted to verify the tool's structural integrity under various load scenarios, reaching up to 19,613 N. The SST was made from ASTM A36 steel, recognized for its mechanical strength and ease of manufacturing. The simulation results demonstrated that the structure stayed within safe limits for both stress and deformation, achieving a minimum safety factor of 1.1. The implementation took place at PT. MPM Hino Yogyakarta, where field testing showed a significant enhancement in technician efficiency. The SST cut down kingpin maintenance time from 360 minutes to only 42.08 minutes, achieving an impressive 88.3% reduction in time spent. Testing for effectiveness, based on feedback from technicians and supervisors, revealed a high level of user satisfaction, particularly in terms of safety, usability, and ergonomic design. The SST tracker kingpin provides a dependable, effective, and secure option for maintaining commercial vehicles. The successful application of it at a Hino service center highlights its practical benefits and the potential for wider implementation throughout the automotive maintenance sector. Additional improvements could involve ergonomic adjustments and the ability to accommodate various truck models, thereby facilitating broader use.

1. Introduction

Transportation plays a vital role in supporting human life, especially in the industrial sector. In Indonesia, the demand for freight transportation continues to increase in line with population growth and economic development. Currently, people not only rely on private vehicles, such as motorcycles and cars, to support their daily activities, but also utilize public transportation, including buses and trucks, for freight transportation [1]. PT. Hino Motors Sales Indonesia (HMSI) and PT. Hino Motors Manufacturing Indonesia (HMMI) is a company that collaborates with Hino Motors to provide vehicles and after-sales services, particularly Hino trucks, which are known for their reliability in the logistics industry [2].

PT. Mitra Pratama Mobilindo Hino Yogyakarta, as part of PT. Sun Motor Group is responsible for distributing and maintaining Hino brand vehicles in the Yogyakarta region. Hino is renowned for the quality and reliability of its products. PT. MPM Hino Yogyakarta, as an official Hino dealer, sells high-quality trucks designed for durability, efficiency, and excellent performance. Hino trucks are engineered to withstand various road conditions and heavy workloads to create a better world through support for safe, economical, and environmentally friendly transportation [3]. Hino is committed to maintaining environmental sustainability by adhering to the principles of sustainable development, in line with the company's vision. Below is the Hino and MPM logo

One of the critical components in this vehicle is the kingpin, which plays a crucial role in safety and driving performance [4-6]. This component determines the vehicle's direction, and if it does not function properly, it can compromise the driver's safety, specifically the steering system. MPM Hino Yogyakarta currently lacks specialized tools or special service tools (SSTs) for handling the kingpin, resulting in slow repair processes that require significant effort and pose risks of damaging other components. This results in prolonged vehicle downtime, which impacts business operations and increases costs. Here is an image of the kingpin component in Fig. 1.

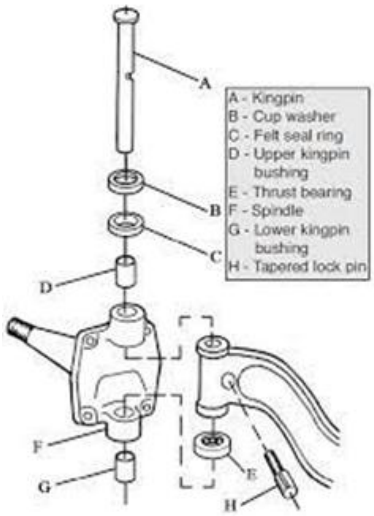

Figure 1. The kingpin component

This issue highlights the urgency of developing specialized SST to facilitate technicians in handling kingpin repairs. Additionally, the absence of kingpin trekker products in the Indonesian market presents a significant opportunity for innovation in this tool, which would not only benefit PT. MPM Hino Yogyakarta also drives changes across the Indonesian automotive industry as a whole. According to Nwanya et al. [7] , the efficient utilization of resources in the manufacturing industry is crucial for minimizing downtime and maximizing productivity. This aligns with PT. MPM Hino Yogyakarta needs to enhance the efficiency of the kingpin repair process. Downtime caused by difficult-to-repair kingpin issues results in operational losses that not only impact efficiency but can also reduce customer satisfaction, as outlined by Patel, Jigar K [8] regarding the importance of preventing equipment damage to reduce downtime.

Meanwhile, Dobromirov et al. [9] emphasize that effective vehicle maintenance is crucial for ensuring safety and optimal performance. The kingpin, as a critical component of the steering system, requires specialized maintenance because damage to this part can affect driving safety. Without adequate SST, technicians must resort to manual methods, such as hammers and chisels, which are not only dangerous but also inefficient, as highlighted by Titu et al. [10] in their emphasis on the importance of using specialized tools for quick and accurate repairs.

Alternative solutions to address this issue involve several approaches. One is to enhance technicians' skills through intensive training to optimize the use of existing tools [11]. However, this approach cannot fully address the issues of time and safety risks. Another alternative is to outsource difficult kingpin repair work to external welding shops, but this only increases costs and extends downtime.

The best solution proposed in this study is to design and develop a kingpin trekker as a specialized SST that can accelerate and secure the repair process. With this tool, technicians will be more efficient in handling repairs, reduce the risk of damaging other components, and shorten vehicle downtime. The development of this SST not only addresses the urgent needs of PT. MPM Hino Yogyakarta also offers innovations that can be applied across the broader automotive industry. This research is urgently needed to provide solutions that directly impact productivity improvements, cost savings, and workplace safety at PT. MPM Hino Yogyakarta, as well as its potential application in the commercial automotive industry in Indonesia.

2. Methodology

This study utilized the Research and Development (R&D) approach, emphasizing the systematic design, creation, and refinement of innovative tools or products aimed at addressing practical problems in real-world contexts. The study utilized the ADDIE development model to structure the development process effectively. This well-known instructional and engineering design framework consists of five interconnected phases: Analysis, Design, Development, Implementation, and Evaluation. Every phase has a distinct purpose to ensure that the tool is both technically sound and user-focused while also being functionally dependable. The ADDIE model was chosen for its iterative approach and capacity to adjust according to ongoing feedback, which makes it especially effective for creating mechanical tools utilized in industrial maintenance. During the Analysis phase, we evaluated the needs of the technicians and the limitations of the current tools. The Design phase included creating technical drawings and running simulations to verify the tool's mechanical integrity. The Development phase concentrated on creating prototypes by utilizing suitable materials and machining methods. During the Implementation phase, the prototype underwent testing in a genuine workshop setting to assess its performance in real-world operational conditions. Finally, the Evaluation phase involved both numerical and descriptive assessments like efficiency testing, user feedback, and structural integrity checks to assess the tool's overall effectiveness and identify areas for improvement.

2.1 Analysis Stage

The analysis phase focused on uncovering the real needs and challenges encountered by technicians in the kingpin maintenance process at PT. MPM Hino Yogyakarta. Observations made in the field, along with organized interviews with workshop personnel, including technicians, foremen, and service advisors, revealed various significant inefficiencies in the existing maintenance workflow. The workshop was particularly lacking a dedicated kingpin puller, leading technicians to use makeshift tools, such as hammers and chisels, instead. This not only prolonged the maintenance period often going beyond six hours but also posed a significant risk of collateral damage to nearby suspension and steering components. The manual removal process also created ergonomic and safety risks for the technicians, particularly during repetitive tasks. The lack of standardized tools resulted in varying maintenance outcomes and a decline in overall service quality. This phase also involved a thorough evaluation of the physical and technical needs of the proposed tool to tackle these issues. We identified key parameters, including operational force, working clearance, material strength, and compatibility with the existing workshop infrastructure. The team recorded the dimensions and limitations of the Hino Series 300 kingpin assembly to guide the design specifications. This groundwork established a crucial foundation for the subsequent design and development phases, ensuring that the final tool would be both effective and tailored to real-world conditions.

2.2 Design Stage

The design phase focused on conceptualizing and intricate modeling of the Special Service Tool (SST) using SolidWorks, a widely recognized 3D computer-aided design (CAD) software commonly employed in precision engineering tasks. This phase converted the initial design requirements identified during the analysis stage into a functional prototype model that considered dimensional accuracy, load-bearing capacity, technician ergonomics, and compatibility with the existing kingpin assembly of Hino Series 300 trucks. The modeling process included several iterations, with each design version undergoing careful review and modifications based on expected mechanical stresses, alignment tolerances, and ease of assembly. Finite Element Analysis (FEA) was performed on the 3D model to assess the structural performance of the tool under simulated real-world operational conditions. The tool underwent load tests varying from 500 kg to 2000 kg, reflecting the anticipated force needed to free a jammed kingpin. The simulations provided insights into Von Mises stress distribution, total deformation, and safety factors, which were crucial for pinpointing critical stress areas and confirming that the tool would withstand the load without failure.

The analysis demonstrated that the SST maintained its structural integrity when subjected to the maximum load, exhibiting acceptable deformation limits and a minimum safety factor of 1.1. The results gave assurance of the tool's mechanical strength. Simultaneously, the selection of materials was carried out with an emphasis on both mechanical strength and manufacturability. The tool components were primarily crafted from ASTM A36 mild steel, chosen for its excellent combination of strength (yield strength of 250 MPa), weldability, and affordability, making it ideal for medium-duty mechanical applications, such as vehicle service equipment. Additionally, design considerations included user ergonomics, focusing on hand placement, accessibility in tight spaces, and ease of alignment during operation, all aimed at reducing technician fatigue and minimizing the risk of injury. This stage resulted in a fully developed digital prototype that satisfied both structural and practical use-case requirements, making it ready to move on to the development and fabrication phase.

2.3 Development Stage

During the development phase, the prototype of the Special Service Tool (SST) was created using the finalized CAD model and the structural simulations that were completed in the design stage. The production activities took place at a local machining and fabrication workshop, Baja Karya, which had the necessary metalworking facilities appropriate for medium-scale tool manufacturing. This stage represented the shift from virtual modeling to actual production, making certain that every design specification could be converted into a real and functional product. The manufacturing process included a series of precise fabrication steps, beginning with the cutting of ASTM A36 steel profiles, plates, and hollow sections to match the component dimensions specified in the engineering drawings. The cut materials were subsequently machined and turned on lathes and milling machines to achieve precise geometries and surface finishes, particularly for critical components such as the housing mount, locking pin shafts, and hydraulic jack seat.

After machining, welding operations were carried out to connect the structural frame, adjuster supports, and reinforcement brackets using arc welding techniques. Attention was given to ensuring the integrity of the welds and proper alignment to uphold the overall strength of the tool and its dimensional accuracy. Next, drilling and tapping processes were performed to create threaded holes for bolt connections and alignment points. After the mechanical assembly was completed, the tool underwent a thorough surface finishing treatment to enhance its durability and visual appeal. This process involved grinding and sanding to remove surface burrs and welding spatter, followed by the application of automotive-grade putty to address minor imperfections. A coat of epoxy primer was applied to enhance corrosion resistance and improve the adhesion of the final paint layer. The finishing process wrapped up with spray painting in industrial yellow enamel paint, selected for its visual appeal and high visibility in workshop settings improving safety and aiding in tool identification.

2.4 Implementation Stage

The implementation phase included deploying and testing the developed Special Service Tool (SST) in a real operational environment at PT. MPM Hino Yogyakarta, utilizing a Hino Series 300 Dutro 110 SD truck that had been diagnosed with kingpin seizure. This phase acted as an essential validation step to evaluate the tool's performance in real service conditions. The testing scenario was designed to replicate the everyday challenges faced by workshop technicians, ensuring the results would apply to regular maintenance tasks. Two comparative procedures for kingpin replacement were conducted to evaluate the tool's effectiveness and efficiency. During the initial procedure, technicians carried out the disassembly using conventional manual tools, including hammers and chisels approaches typically employed when specialized equipment is unavailable. During the second procedure, the same technicians performed the replacement with the newly developed SST. This system featured a 2-ton hydraulic bottle jack that was integrated into a guided pulling mechanism, allowing for the safe extraction of the kingpin with minimal manual effort.

During the trials, technicians recorded the total time needed for each method by following standardized timing protocols. Furthermore, qualitative observations were made on several important aspects: (1) usability, which encompassed ease of operation, alignment precision, and ergonomic comfort; (2) safety, which emphasized the reduction of physical strain and the risk of component damage; and (3) time efficiency, measured by comparing the durations of both procedures. The test results showed a significant decrease in service time from about 360 minutes (6 hours) with traditional methods to just 42.08 minutes using the SST indicating an improvement in time efficiency of more than 88%. Additionally, utilizing the SST eliminated the need for continuous hammering, which reduced the risk of injury and prevented accidental damage to nearby components, such as bushings, axles, and suspension brackets.

2.5 Evaluation Stage

The evaluation phase aimed to thoroughly examine both the functional performance and user perception of the Special Service Tool (SST) created for kingpin removal on Hino Series 300 trucks. This phase was carefully divided into two primary components: efficiency testing and effectiveness testing, with each focused on validating distinct aspects of the tool's performance. For the efficiency assessment, we gathered quantitative data by comparing the total time taken to complete the kingpin replacement task using two different methods: (1) the traditional manual approach and (2) the SST-assisted approach. The results showed a significant reduction in task duration, with the traditional process taking around 360 minutes, while the SST-assisted procedure finished in only 42.08 minutes. The significant time difference of over 320 minutes, representing an 88% reduction, highlights the SST's ability to minimize downtime and significantly improve service throughput in workshop settings.

A structured questionnaire was created and sent out to three participants for the effectiveness assessment: two seasoned technicians and one foreman, all of whom played a direct role in the testing process. The questionnaire utilized Likert-scale and Guttman-scale tools to assess the level of agreement and binary performance evaluations across various key indicators. Factors considered included the availability of tools, user-friendliness, safety during operation, mechanical dependability, ergonomic design, and the perceived quality of construction. The Likert-scale results indicated an apparent inclination towards positive responses, as most indicators were rated as "Agree" or "Strongly Agree." This demonstrates a strong sense of user satisfaction, particularly regarding the tool's practical usability and intuitive handling in the field. In the meantime, the Guttman-scale analysis, which concentrated on Yes/No responses regarding technical performance and durability, achieved a flawless affirmative score of 100%. This result indicates a strong consensus among users that the tool met or exceeded all operational expectations.

Additionally, user feedback highlighted that the SST offered a more controlled, safer, and physically efficient option compared to the earlier manual method. Participants observed that the tool reduced the need for brute force, enhanced technician posture during use, and helped prevent possible damage to nearby components, such as axle housing and bushings. The results clearly showed that the SST enhanced both quantitative efficiency metrics and received positive qualitative feedback from the end users. Following a thorough dual evaluation, the tool was found to be technically effective and ready for field use, showing promise for broader integration into commercial vehicle maintenance processes.

3. Result and Discussion

3.1 Design of special service tools tracker kingpin

The unique kingpin tracking tool's design is depicted in Fig. 2. Aside from the main frame and top cover, there are seven more important parts: the frame adjuster, the hydraulic jack bottle, the seven-pin locking pin, the bottom cover, and the kingpin store. As you work to maintain the kingpin, each part is engineered to give you the assistance and functionality you need. In order to maintain stability and strength while it is in operation, the main frame serves as the principal structural support. To keep the kingpin housing in place and stable while the hydraulic jack applies pressure, the top cover is fastened. With the help of the frame adjuster, you can position and align the tool with pinpoint accuracy, making it easier to use and more precise. Aside from that, while the kingpin is being removed, it is securely housed in the kingpin storage. The tool is designed with a locking pin to prevent the kingpin from moving accidentally, a hydraulic jack bottle to provide the powerful mechanical force needed to remove it, and an M17 bolt to secure everything together, making it reliable and safe.

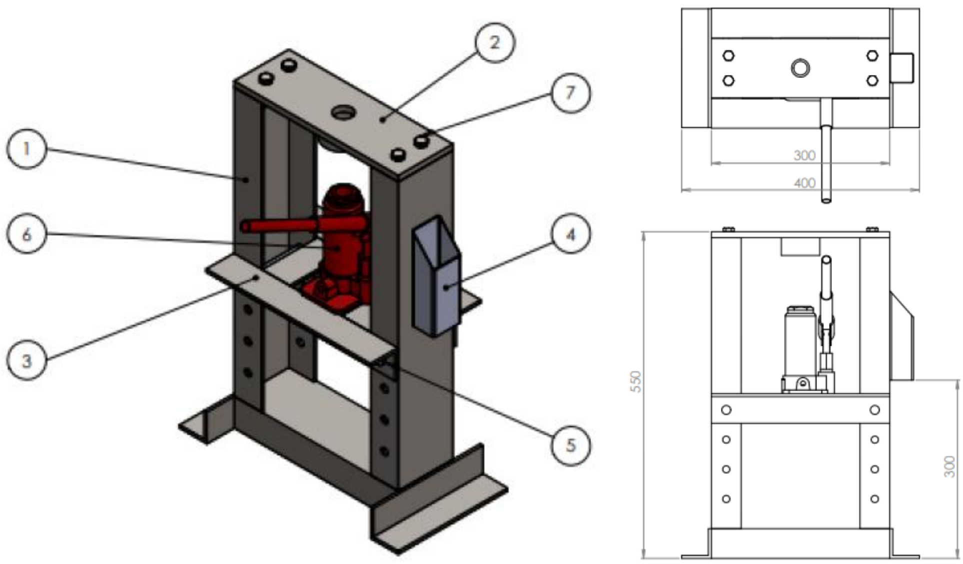

Figure 2. Design special service tools tracker kingpin

Table 1 shows the component name of the special service tools tracker kingpin. The main frame design of this tool serves as a support for the frame adjuster and jack. This main frame is made of 10mm thick UNP 100 iron and measures 200 x 400 x 550. The height of this main frame is 55 cm. The selection of UNP 100 material was made because it has high strength and durability, is capable of withstanding heavy loads, and is resistant to deformation and external pressure. With its sturdy structure, the main frame ensures the device's overall stability, enabling it to operate safely and efficiently under various working conditions.

The top cover functions as a kingpin retainer when the jack is in operation. This top cover is equipped with four 17 mm bolt holes to connect the top cover to the main frame. The Top Cover is made of a 1 mm thick steel plate with dimensions of 400 mm in length, 40 mm in height, and 100 mm in width. A 10 mm thick steel plate is chosen to ensure strength and stability during operation, thereby reducing the risk of deformation or damage when bearing loads. This design is also engineered to facilitate assembly and disassembly, thereby simplifying maintenance.

The frame adjuster is used to adjust and set the frame position to suit the needs and specifications of the tool being used. This ensures that the frame remains stable and precise during operation, thereby improving work efficiency and safety. With maintained precision, the frame adjuster also helps reduce the risk of errors in tool operation, provides comfort for technicians while working, and minimizes potential damage to other components. The frame adjuster is made from high-quality angle iron measuring 50 x 50 x 5 mm with a length of 400 mm, providing optimal strength and durability for long-term use.

Table 1. Component names special service tools tracker kingpin

No	Part name	Material	Dimension	Quantity
1	Main Frame	Standard	200 x 400 x 550	4
2	Top Cover	Iron Plate	40 x 100 x 300	1
3	Frame Adjuster	Angle Iron	50 x 202 x 300	1
4	Storage Kingpin	Hollow Iron	40 x 50 x150	1
5	Locker Pin	Solid Iron	Ø15 X 135mm	2
6	Jack Hydraulic Bottle 2 Ton	Standard	2 TON	1
7	Bolt M17	Standard	M17	4

This storage kingpin is designed as a special container for storing kingpins that are to be replaced or used kingpins that have been removed using special service tools. This storage kingpin is designed to ensure the safety and cleanliness of the kingpin during storage, thereby reducing the risk of contamination or damage to kingpins that will be reused. The tool is made from high-quality 5mm angle iron, providing the structure with strength and stability. The dimensions of the storage kingpin are as follows: a side width of 40 mm, a front width of 50 mm, and a height of 150 mm. This design provides sufficient space while remaining compact and easy to integrate into the work environment.

This locker pin serves as a lock for the frame adjuster, which is connected to the main frame. The locker pin is made of solid iron with a diameter of 15 mm at the head and 10 mm for the body. The locker pin measures 135 mm in length. The selection of solid iron as the primary material ensures high durability, capable of withstanding the pressure and forces that arise during operation without risk of failure [12, 13]. Its precise design also allows for quick installation and removal, facilitating adjustments or routine maintenance. This is crucial for maintaining the tool's overall performance and ensuring safety during use.

3.2 Simulation results of special service tools tracker kingpin

The results of design simulations with various load variations, namely 4903 N, 9806 N, 14709 N, and 19613 N. These simulations were conducted to analyze the structure's response to the applied loads, including stress values, deformation, and the resulting safety factors. The material used was ASTM A36.

This locker pin serves as a lock for the frame adjuster, which is connected to the main frame. The locker pin is made of solid iron with a diameter of 15 mm at the head and 10 mm for the body. The locker pin measures 135 mm in length. The selection of solid iron as the primary material ensures high durability, capable of withstanding the pressure and forces that arise during operation without risk of failure. Its precise design also allows for quick installation and removal, facilitating adjustments or routine maintenance. This is crucial for maintaining the tool's overall performance and ensuring safety during use.

Fig. 3a shows that the structure undergoes deformation of 566.277 mm and stress of 55.42 MPa under a load of 4903 N, as shown in the simulation results. The simulation yielded a safety factor of 4.5, as shown in Fig. 3b. These results demonstrate that the intended structure can reliably withstand operational loads without any structural damage. Although there is quantifiable deformation, it remains within the tolerated limit, indicating that the structure is stable under the projected operating conditions. In addition, the tool has a strong margin of strength, as indicated by its high safety factor, which means it can safely handle additional stresses above the tested load. That the specialized kingpin tracking gadget will last and work as intended when used in actual car repair procedures is reassuring.

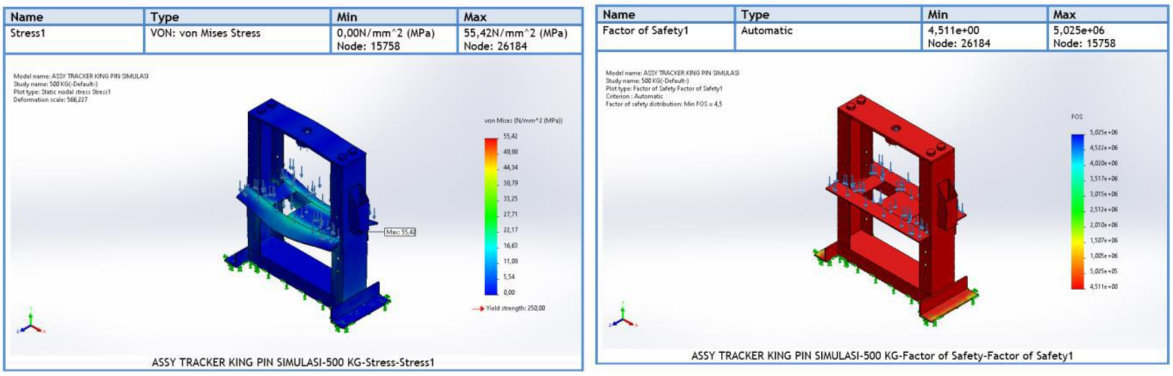

Figure 3. Simulation results at a load of 4903 N: a) Stress and b) Safety factor

The structure experiences a stress of 110.84 MPa and a deformation of 283.114 mm under a load of 9806 N, as shown in Fig. 4. This simulation yielded a safety factor of 2.3. This safety factor indicates that the tool's structural integrity remains adequate, even though there is less room for extra loading than in the lower load situation previously. There is a notable decrease in deformation at this higher load, indicating enhanced structural stiffness and efficient force distribution, even if the stress levels are significantly higher.

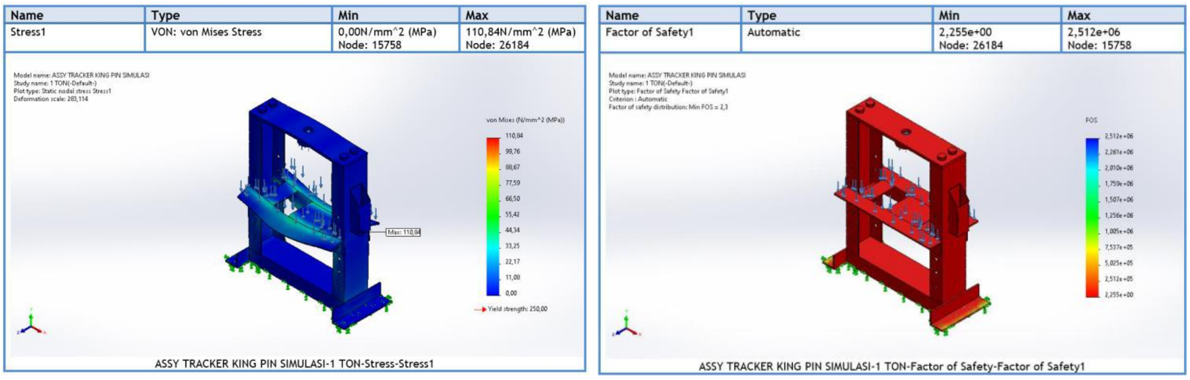

Figure 4. Simulation results at a load of 9806 N: a) Stress and b) Safety factor

Fig. 5 indicates that when the load is 14,709 N, the structure is under stress of 166.26 MPa and is deformed by 188.742 mm. The simulation gives us a safety factor of 1.5. This number shows that the structure can still handle the weight with a respectable level of safety. However, the margin is smaller than it would be with a lower load. The deformation observed is acceptable and does not impact the tool's performance or alignment when in use. However, the fact that the safety factor decreases as the load increases indicates that using something near this load threshold for an extended period or repeatedly should be done with caution.

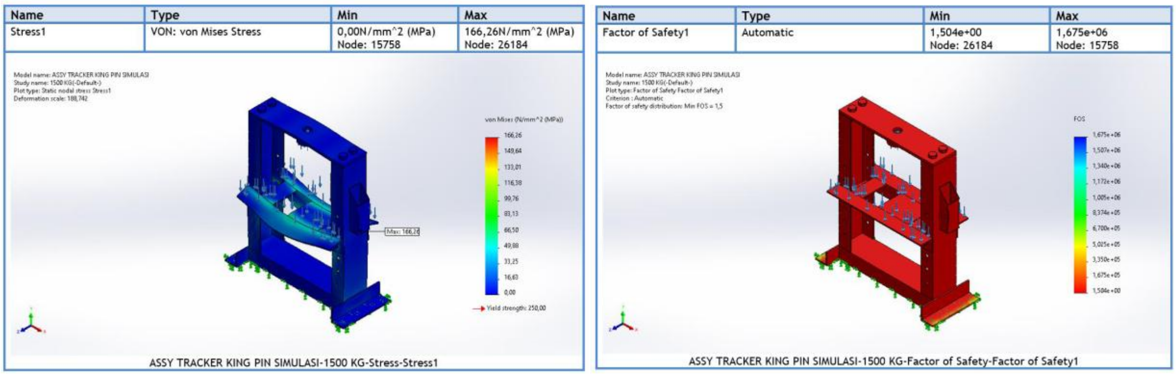

Figure 5. Simulation results at a load of 14709 N: a) Stress and b) Safety factor

The simulation results reveal that the structure undergoes a stress of 221.68 MPa and a deformation of 141.557 mm under a load of 19,613 N, as shown in Fig. 6. Fig. 6b shows the safety factor that was achieved from this simulation, which is 1.1. This number indicates that the structure is likely to be unable to withstand much more stress before it breaks. Although the distortion is still below permissible limits, structural collapse or permanent deformation could occur with any additional increase in load due to the low safety factor.

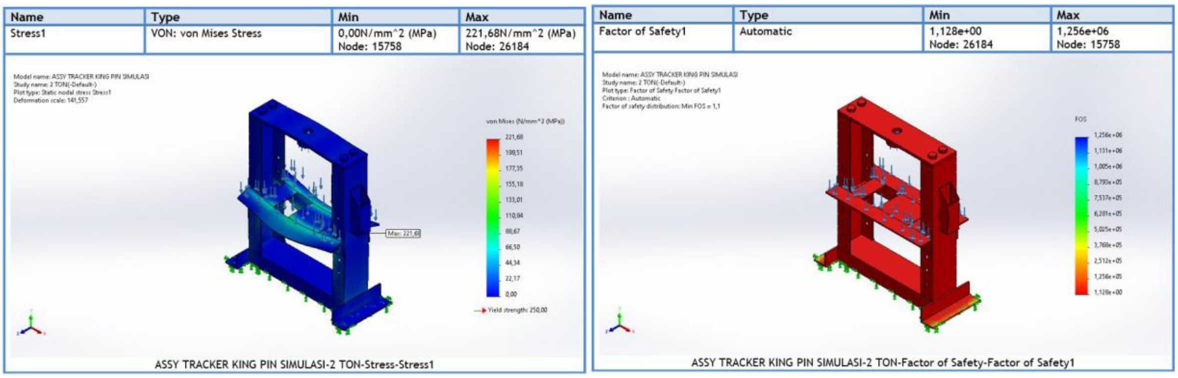

Figure 6. Simulation results at a load of 19613 N: a) Stress and b) Safety factor

The kingpin of the special service tool tracker prototype is shown in Fig. 7a. Pressing down on the jack lever causes resistance, which is used to detect the kingpin application of the testing tool (Fig. 7b). Fig. 7c shows the results of the successful testing of the special tracker kingpin tool, which proved to help handle stuck kingpin components. This demonstrates that the hydraulic jack mechanism can generate sufficient force to disassemble components that are often difficult to remove by hand. Moreover, the tool's structural integrity remained unaltered throughout the procedure, demonstrating its reliability and endurance under operational stress. The test's positive results demonstrate that the SST can reduce time, effort, and risk during kingpin removal operations, thereby significantly improving maintenance procedures.

(a)

(b) (c)

Figure 7. Special service tools tracker kingpin: a) prototype, b) and c) prototype testing

The simulation results from the special service tools tracker kingpin offer important insights into how the tool behaves structurally and its mechanical limits when subjected to different load conditions. The structure was evaluated through Finite Element Analysis (FEA) under loads of 4903 N, 9806 N, 14,709 N, and 19,613 N, reflecting a variety of realistic operational stresses faced during kingpin maintenance. With a minimum load of 4903 N, the observed stress was 55.42 MPa, resulting in a deformation of 566.277 mm and a safety factor of 4.5. The impressive safety factor highlights the tool's strong structural redundancy and durability during light to moderate use, ensuring it can handle occasional overloading without issue.

With the increase in load, a clear pattern emerged: stress and deformation escalated, whereas the safety factor diminished. At 9806 N, the tool underwent a stress of 110.84 MPa and a deformation of 283.114 mm, resulting in a safety factor of 2.3, which remains within acceptable limits for mechanical operations. At 14,709 N, the stress rose to 166.26 MPa, the deformation fell to 188.742 mm, and the safety factor decreased to 1.5. Even though the structure continued to function, this decreasing safety margin indicates a point at which ongoing use might jeopardize its long-term dependability. Under the highest load tested at 19,613 N, the stress reached a maximum of 221.68 MPa, accompanied by a deformation of 141.557 mm, leading to a safety factor of only 1.1. This value, although still above the critical limit, suggests that the tool is nearing its yield point and should not be regularly employed in such extreme conditions.

The results of these simulations indicate that the SST design is mechanically robust under standard operating loads and possesses adequate durability for practical use. They emphasize the need to establish a safe working load limit for regular use to prevent fatigue or structural failure in the long run. The decreasing safety factor at increased loads highlights the importance of establishing appropriate usage guidelines and regular inspection routines. In summary, the simulation confirms that the SST tracker kingpin is a dependable, high-strength tool designed for medium-duty service tasks, ensuring both operational safety and performance efficiency.

3.3 Efficiency of special service tools tracker kingpin

Efficiency testing was carried out to measure the improvement in work efficiency gained by using Special Service Tools (SST) for kingpin trekkers in comparison to traditional manual methods. The testing was conducted at PT. Mitra Pratama Mobilindo Hino Yogyakarta, utilizing a Hino Series 300 Dutro 110 SD unit that had been identified with kingpin problems. Two distinct methods were employed for the kingpin replacement task: the first involved traditional tools and techniques, such as hammers and chisels. At the same time, the second made use of the specially developed SST tracker kingpin.

The findings showed a significant variation in performance between the two methods. The conventional approach took approximately 360 minutes (6 hours) to complete the kingpin replacement, underscoring its lengthy and labor-intensive nature. On the other hand, utilizing the SST allowed the same procedure to be completed in just 42.08 minutes. This represented a significant decrease of 320 minutes, translating to an 88.3% enhancement in time efficiency. This significant reduction enhances productivity in the workshop while also reducing vehicle downtime, enabling commercial units to return to work more quickly and improving service delivery to customers.

Additionally, utilizing the SST greatly reduces the physical strain on technicians by eliminating repetitive, labor-intensive tasks, such as hammering. This enhances occupational health and safety, reducing the likelihood of work-related injuries and technician fatigue. In addition to the numerical assessment of efficiency, it was crucial to confirm the tool's performance in real-world scenarios. As a result, effectiveness testing was carried out by distributing structured questionnaires to the technicians and supervisors participating in the trial. The assessment centered on three main areas: the tool's availability when required, its operational performance during kingpin removal, and the overall quality of construction and ergonomics. The gathered feedback provided important insights into user satisfaction and validated the tool's reliability and usefulness in the field.

4. Conclusion

The kingpin components of Hino Series 300 trucks were the focus of this study's successful development of a Special Service Tool (SST). A systematic approach was ensured throughout the development process, from analysis to assessment, by following the ADDIE methodology. Using SolidWorks for initial design and modeling, the instrument was then structurally validated through Finite Element Analysis (FEA) to assess its mechanical performance under various loading conditions. The material that was chosen, ASTM A36 steel, is ideal for medium-duty automotive maintenance applications due to its cost-effectiveness, machinability, and attractive strength-to-cost ratio. With stress and deformation values kept within acceptable ranges, the tool was found to be capable of securely withstanding operational loads up to 19,613 N, according to the simulation results. The tool's structural integrity and appropriateness for actual field use in high-stress settings were confirmed by the minimum recorded safety factor of 1.1 under maximum load conditions. A Hino Series 300 Dutro 110 SD unit was used for field testing at PT. MPM Hino Yogyakarta to assess the tool's performance in real-world conditions. A remarkable time savings of around 88.3% was achieved by the SST, which reduced the kingpin replacement time from 360 minutes to just 42.08 minutes, demonstrating a significant improvement in technician labor efficiency. By eliminating potentially harmful manual procedures, such as hammering, the instrument enhanced technician safety and reduced the risk of damage to nearby components, including axle housings and bushings. The tool's practical efficacy in a workshop setting is further supported by the significant favorable reactions to its usability, operational safety, ergonomic design, and durability, as indicated in the user feedback obtained through structured questionnaires. Ultimately, the developed SST tracker kingpin is an efficient, safe, and sturdy solution that addresses critical issues in commercial truck maintenance. It enhances uniformity in repair results, increases job safety, and reduces labor time without compromising service quality. Thanks to its effective deployment at PT. MPM Hino Yogyakarta, this product is already useful for Hino's service networks. The design may not be perfect, but it is adaptable and efficient, offering hope for its widespread adoption in the truck repair sector. Improving the tool's adaptability to different vehicle types, making it more ergonomic to lessen technician weariness, and investigating scalable manufacturing methods for nationwide distribution and mass production should be the priorities of future development.

Conflict of interest

The authors declare no conflict of interest.

References

[1] D. Carracedo and H. Mostofi, "Electric cargo bikes in urban areas: A new mobility option for private transportation," *Transportation Research Interdisciplinary Perspectives,* vol. 16, p. 100705, 2022, doi: https://doi.org/10.1016/j.trip.2022.100705.

[2] B. Zwolińska and J. Wiercioch, "Modelling the Reliability of Logistics Flows in a Complex Production System," *Energies,* vol. 16, no. 24, p. 8071, 2023, doi: https://doi.org/10.3390/en16248071.

[3] D. A. Hensher and E. Wei, "Energy and environmental costs in transitioning to zero and low emission trucks for the Australian truck Fleet: An industry perspective," *Transportation Research Part A: Policy and Practice,* vol. 185, p. 104108, 2024, doi: https://doi.org/10.1016/j.tra.2024.104108.

[4] D. Nagaraju, "Fundamentals and Challenges of Conventional Road Transportation," in *The Future of Road Transportation*: CRC Press, 2023, pp. 1-28.

[5] J. Käsgen, J.-P. Kobler, and R. Möller, "Kingpin load measurement of a semi-trailer," 2022: Springer, pp. 226-245, doi: https://doi.org/10.1007/978-3-658-40783-4_16.

[6] G. Xu, W. He, F. Chen, H. Shen, and X. Li, "One-dimension orientation method of caster and kingpin inclination of vehicle wheel alignment," *Measurement,* vol. 198, p. 111371, 2022, doi: https://doi.org/10.1016/j.measurement.2022.111371.

[7] S. C. Nwanya, J. I. Udofia, and O. O. Ajayi, "Optimization of machine downtime in the plastic manufacturing," *Cogent Engineering,* vol. 4, no. 1, p. 1335444, 2017, doi: https://doi.org/10.1080/23311916.2017.1335444.

[8] J. K. Patel, "The importance of equipment maintenance forecasting," *Int. J. Mech. Eng,* vol. 8, no. 5, pp. 7-11, 2021, doi: 10.14445/23488360/IJME-V8I5P102.

[9] V. Dobromirov, V. Verkhorubov, and I. Chernyaev, "Systematizing the factors that determine ways of developing the vehicle maintenance system and providing vehicle safety," *Transportation research procedia,* vol. 36, pp. 114-121, 2018, doi: https://doi.org/10.1016/j.trpro.2018.12.052.

[10] A. M. Titu, D. Grecu, A. B. Pop, and I. R. Șugar, "Service Process Modeling in Practice: A Case Study in an Automotive Repair Service Provider," *Applied Sciences,* vol. 15, no. 8, p. 4171, 2025, doi: https://doi.org/10.3390/app15084171.

[11] R. Srivastava, M. Awojobi, and J. Amann, "Training the Workforce for High-Performance Buildings: Enhancing Skills for Operations and Maintenance," *American Council for an Energy-Efficient Economy, Washington, DC,* 2020.

[12] D. Raabe, "The materials science behind sustainable metals and alloys," *Chemical reviews,* vol. 123, no. 5, pp. 2436-2608, 2023.

[13] M. A. Maleque and M. S. Salit, *Materials selection and design*. Springer, 2013.

JOURNAL OF AUTOMOTIVE AND MECHANICAL APPLIED TECHNOLOGY

Vol. 2 No. 1, 2025, pp. 124-131 https://journal.uny.ac.id/publications/jamat https://doi.org/10.21831/jamat.v2i1.1779

Engineering Design and Performance Evaluation of a Transmission System for the UG 24 Urban Energy Vehicle

Muhammad Farid Riyanto[1], Juni Noor Rohman[2], Sutiman[3*]

[1]Department of Mechanical and Automotive Engineering, Faculty of Vocational, Universitas Negeri Yogyakarta, Kulon Progo, Yogyakarta 55652, Indonesia
[2]Graduate Program Student Mechanical Engineering, Wrocław University of Science and Technology, Poland
[3]Department of Automotive Engineering Education, Faculty of Engineering, Universitas Negeri Yogyakarta, Sleman, Yogyakarta 55281, Indonesia

*Corresponding author: sutiman@uny.ac.id

ARTICLE INFO

Article history:
Received 09.05.2025
Revised 05.06.2025
Accepted 30.06.2025

Keywords:
Transmission System; Energy-Efficient Vehicle; Student Innovation; 4D Method; Custom Design.

ABSTRACT

The development of energy-efficient vehicles in student competitions encourages innovation in lightweight and high-performance automotive systems. The Garuda UNY Team, representing Universitas Negeri Yogyakarta, has been actively involved in national competitions such as the Kontes Mobil Hemat Energi (KMHE). In recent evaluations, the team identified a critical weakness in their vehicle's drivetrain, specifically the Internal Gear Hub (IGH) used in the UG-24, which failed to withstand engine torque during acceleration, leading to gear slippage and mechanical failure. To address this issue, a new transmission system was designed and manufactured using the 4D development framework: Define, Design, Develop, and Disseminate. The Define phase identified the mismatch between the IGH design and engine torque requirements. In the Design phase, a new gearbox layout was modeled using Autodesk Inventor, incorporating components such as a crankcase, cover, and custom gear ratios. The development phase involved selecting materials, laser cutting, machining, and assembling transmission parts from mild steel and aluminum. Finally, the Dissemination phase consisted of installing the system in the UG-24 vehicle and conducting a performance evaluation through structured interviews with drivers. Evaluation results showed improved gear shifting performance, with a 75% success rate across ten indicators. Despite positive outcomes, some issues, such as shifting resistance and gear engagement noise, were observed. These were linked to cable friction and dog clutch geometry. Design improvements such as optimized routing and chamfering were recommended for future iterations. This research highlights the impact of tailored transmission systems in student-built energy-efficient vehicles. It provides insight into practical, scalable drivetrain solutions.

1. Introduction

Student organizations play a crucial role in fostering students' interests and talents across various disciplines, including science and technology [1]. At Universitas Negeri Yogyakarta (UNY), one of the most prominent organizations in engineering development is the Technology Engineering Student Organization (UKM Restek), which houses several divisions, including the Garuda UNY Team. This team focuses on research and development in the field of fuel-efficient and high-performance vehicles, applying engineering principles and knowledge gained during the academic process. Over the years, the Garuda UNY Team has actively participated in both national and international competitions such as the Shell Eco-marathon, Student Formula Japan, and the Energy Efficient Car Contest (KMHE), a highly competitive annual event in Indonesia [2].

In participating in the KMHE competition, the Garuda UNY Team has encountered various technical challenges that hindered its ability to achieve the targeted fuel efficiency of 700 km/liter. Based on internal evaluations, several key factors were identified: aerodynamic drag resulting from the body design, excessive friction in the braking system, chassis deflection due to uneven load distribution, and transmission system failure caused by an inability to handle engine torque [3, 4]. Notably, the Internal Gear Hub (IGH) transmission system, initially designed for bicycles, proved to be inadequate for use in an urban concept vehicle due to its inability to transfer power under high-torque conditions [5] efficiently.

From an engineering perspective, the failure of the IGH transmission system highlights a mismatch between component specifications and the vehicle's torque requirements. A transmission not designed to handle high torque and dynamic loads is prone to deformation or mechanical failure [5]. Furthermore, suboptimal gear ratios negatively affect acceleration and energy efficiency [6]. Previous studies recommend that energy-efficient vehicle transmissions should be designed to maximize torque transfer efficiency, minimize internal friction, and utilize lightweight yet robust materials and structures [7, 8].

This issue is further exacerbated by spatial limitations within the urban vehicle's chassis, which demands a compact and precisely integrated transmission system. Key factors, such as material selection, housing design, and assembly techniques, must be carefully considered to avoid new issues, including vibration or misalignment of the drivetrain [7, 9]. Without a well-engineered design, even newly developed systems may compromise driving performance or comfort. Therefore, a systematic engineering approach is required to develop a new transmission system that ensures optimal power transfer, structural reliability, and spatial efficiency.

To address these challenges, this study proposes the design and fabrication of a custom transmission system tailored specifically to the needs of the Garuda UNY Team's urban vehicle. The proposed system is developed based on real torque requirements, spatial constraints, and operational ergonomics. It is expected that this new design with improved structural strength, precision, and optimal gear ratios will significantly enhance both vehicle acceleration and energy efficiency. This research not only aims to provide a technical solution for the team's current limitations but also contributes to the broader field of sustainable mobility and energy-efficient vehicle development in Indonesia.

2. Methodology

2.1 Design Procedure

This study employs a Research and Development (R&D) approach combined with the 4D model development stages: Define, Design, Develop, and Disseminate [10]. At the Define stage, the research team identified the critical problem in the UG 24 vehicle, specifically the inability of the Internal Gear Hub (IGH) transmission to withstand the high engine torque, which caused frequent system failures. Recognizing this limitation became the basis for developing a new, more robust transmission system to enhance the vehicle's acceleration performance.

During the Design stage, the transmission system components were modeled using the SolidWorks software. The design focused on several key parts, including the Crankcase, Crankcase cover, Input and output gears, Shift drum, Shift forks, and Bushing bearings. The design aimed to optimize space constraints within the urban vehicle chassis, ensuring precise gear meshing to reduce backlash and improve transmission efficiency. To determine the appropriate gear ratios for each transmission stage, Equation 1 was used to calculate the maximum velocity based on wheel diameter and gear ratio.

$$v = \frac{\pi \cdot D_w \cdot 60 \cdot RPM}{1000 \cdot r_{total}} \quad (1)$$

Where : v = Average speed
D_w = Wheel diameter
r_{tot} = Total gear ratio

At the Development stage, the transmission components were custom-manufactured in a workshop setting. Processes such as laser cutting for crankcase fabrication, turning for bushing bearing creation, and milling for precision adjustments were employed to bring the design to life. The manufacturing process prioritized the use of lightweight yet durable materials to enhance the overall vehicle performance while maintaining structural integrity.

Finally, the Disseminate stage involved functional testing and evaluation of the developed transmission. Road tests were conducted alongside interviews with the drivers to gather qualitative feedback on the ease of gear shifting, operational smoothness, and ergonomic considerations of the gear shifter. This stage ensured that the transmission system met performance expectations and could be effectively integrated into future competition vehicles.

3. Result and Discussion

3.1 Final product design

Fig. 1 shows the final design of the transmission. The transmission system developed in this study utilized a combination of materials selected for their mechanical strength, durability, and lightweight properties, thereby optimizing vehicle performance. The crankcase (Fig. 2) was fabricated from mild steel sheets with a thickness of 4 mm, chosen for its balance between strength and weight, ensuring robust protection for internal components while minimizing additional mass. The transmission gears, including input, output, and intermediate gears, were manufactured from alloy steel known for its high tensile strength and wear resistance, which is essential for withstanding the high torque loads during acceleration.

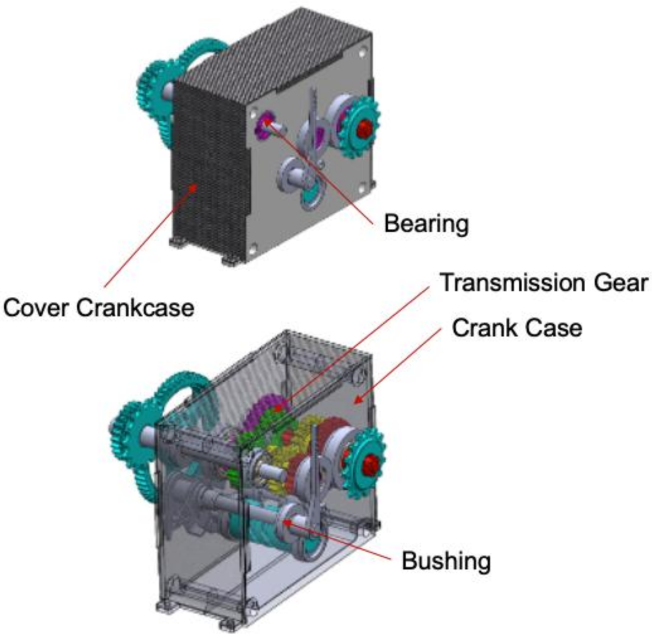

Figure 1. 3D design of transmission

Bearings and bushings were incorporated to reduce friction between rotating parts and maintain precise alignment of gear shafts [11]. Specifically, bronze bushings were chosen for their excellent load-bearing capacity and self-lubricating properties. At the same time, ball bearings made of hardened steel were selected for their ability to sustain both radial and axial loads. The assembly process involved precise machining to ensure tight tolerances, reducing backlash and improving the efficiency of power transmission.

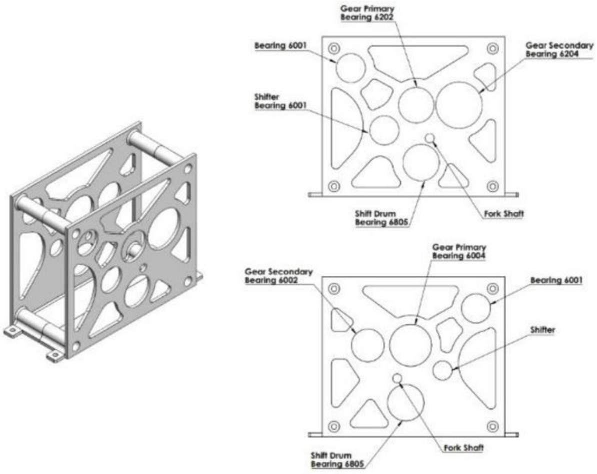

Figure 2. 3D design of crankcase component

The setup phase involved assembling all components within the limited space of the urban vehicle chassis. Special attention was given to the alignment of the crankcase and mounting points to ensure a secure fit within the vehicle frame, without compromising space or interfering with other systems. The gear-shifting mechanism, including the shift drum and forks, was calibrated to ensure smooth and accurate gear transitions [12]. Autodesk Inventor software was extensively used throughout the design and assembly process to simulate component fit and movement, thereby minimizing errors before physical manufacturing and assembly.

3.2 Manufacturing and assembly process

The manufacturing stage marks a critical transition from design to realization, involving the fabrication of individual transmission components and their precise assembly into a functional system. All components were custom-manufactured according to the CAD model specifications, with a focus on optimizing spatial constraints and structural integrity for the Urban Concept vehicle.

Figure 3. The component of transmission

Fig. 3 illustrates the complete set of transmission parts after the fabrication process. Key components include the crankcase, gear sets, bushing units, shafts, and the transmission cover. These parts were produced using a combination of laser cutting and CNC machining techniques, with materials selected to balance strength and weight, primarily mild steel for structural frames and aluminum T7 for lighter housing components. Each part was subjected to dimensional inspection to ensure fit tolerance, especially for rotating components such as bearings and shafts.

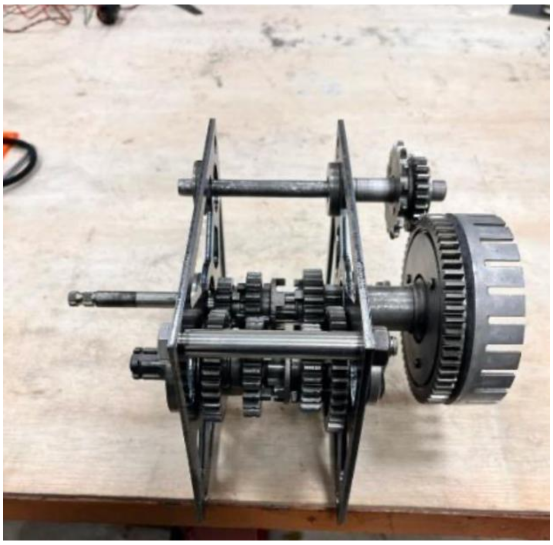

Figure 4. Assembly of transmission

Following fabrication, the assembly process was initiated. Fig. 4 shows the integration of all transmission components into a single unified system. This phase required high precision in aligning the input shaft, intermediate gears, and output shaft, as well as the installation of bushings and bearing seats. Proper alignment was critical to avoid backlash and ensure efficient torque transmission. Lubrication was applied to all contact surfaces to minimize friction during operation [13, 14].

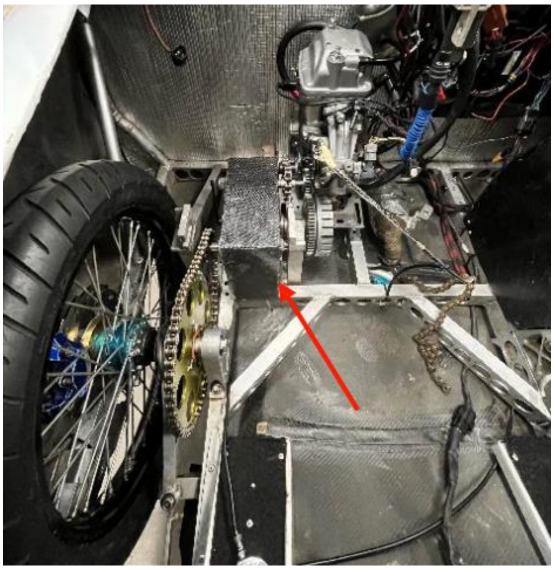

Figure 5. Installation of transmission on the chassis

Once assembled, the transmission unit was installed into the Urban Concept vehicle chassis, as shown in Fig. 5. The positioning of the transmission system was constrained by the existing IGH mounting space, which necessitated design adaptations to ensure compatibility. Special attention was given to the chain tension and alignment between the input gear and final drive [15]. The system was bolted securely to the vehicle frame, and a preliminary setting was conducted to check clearance and ensure smooth movement of the chain drive under load. This manufacturing and assembly workflow ensured that the final product was robust, functional, and tailored for real-world implementation on the Garuda UNY UG 24 vehicle. The success of this stage laid the groundwork for further testing and refinement in the performance evaluation phase.

3.3 Transmission system performance evaluation

The performance evaluation of the developed transmission system was conducted using a qualitative approach, involving a structured interview form. Two experienced drivers from the Garuda UNY Team were involved in the testing phase to assess the functionality and ergonomics of the transmission during actual vehicle operation. The evaluation focused on ten key indicators, including ease of gear shifting, gear engagement smoothness, the presence of unusual noises or jerking, and ergonomic factors such as gear lever accessibility and shifting effort.

Table 1. Evaluation result or the transmission

No.	Evaluation Criteria	Driver 1	Driver 2	Remarks
1	Ease of gear shifting	Yes	Yes	Gear shifting can be executed smoothly without excessive force.
2	Noise during acceleration	Yes	No	Noticeable gear noise is present
3	Shifting consistency across speeds	Yes	Yes	Smooth transition across all speed ranges, except minor resistance at higher speeds.
4	Presence of vibration or jerking	Yes	Yes	Slight jerking occurs during shifting due to the lack of a synchromesh system.
5	Transmission responsiveness during acceleration	Yes	Yes	Transmission remains responsive and consistent under acceleration.
6	Gear lever obstruction	Yes	Yes	The gear lever path is slightly obstructed due to suboptimal cable routing.
7	Accessibility of the gear lever	Yes	Yes	The lever position is ergonomically reachable and does not hinder operation.
8	Ease of returning to neutral	Yes	Yes	The neutral position is easily identifiable in all conditions.
9	Gear slippage	No	No	No slippage detected during normal operation.
10	The effort required for shifting	Yes	Yes	Gear shifting does not require excessive force; it operates within ergonomic limits.

Based on the structured form, each driver was asked to provide their feedback by answering "Yes" or "No" to each question, which was designed to reflect real-time driving conditions during acceleration, deceleration, and cruising. The criteria also addressed potential issues such as gear slippage and difficulties in returning to the neutral position.

From the initial feedback shown in Table 1, the drivers reported that the gear shifting process could generally be executed smoothly, with the gear lever easily reachable and operable without excessive force. However, both drivers noted the presence of a slight jerking sensation and a coarse sound when shifting from gear two to gear three. This issue is likely caused by the use of a constant mesh (non-synchronized) transmission system, which lacks a synchromesh mechanism to harmonize gear and shaft speeds prior to engagement.

Furthermore, minor resistance was observed in the gear lever's movement, particularly due to the suboptimal routing of the cable mechanism, which resulted in increased friction. This suggests a need for future optimization in the cable arrangement and selection of more flexible materials to enhance responsiveness and user comfort [16]. In general, the evaluation showed that 75% of the performance indicators were met satisfactorily, indicating that the developed transmission system functions effectively and is suitable for use in competition.

Nonetheless, several areas have been identified for improvement, including the refinement of gear engagement surfaces and the enhancement of cable mechanism ergonomics.

3.4 Weakness analysis and improvement

Based on the evaluation results and observations during the transmission testing phase, several weaknesses were identified in the newly developed transmission system. These weaknesses are important to analyze in order to provide constructive insights for future improvements. The first noticeable issue was the presence of harsh noise and vibration, particularly when shifting from the second to the third gear. This symptom is indicative of impact engagement caused by the non-synchronized nature of the constant mesh transmission. Without a synchromesh mechanism, the gear and shaft rotations are not equalized before engagement, resulting in abrupt contact [17]. This condition leads to discomfort and potential long-term mechanical wear. To address this issue, a redesign of the dog clutch geometry is proposed, incorporating chamfering or tapering on the gear teeth. This technique smoothens the engagement process by allowing gradual contact between gear teeth, thereby reducing the impact force and enhancing shifting comfort.

Another observed weakness involves the gear shifter cable system. During testing, the shift lever occasionally exhibited resistance, which disrupted the smoothness of gear changes. This problem is attributed to suboptimal routing of the cable and excessive curvature, which increases friction and hampers responsiveness. Improvement can be achieved by optimizing the cable routing layout, minimizing unnecessary bends, and possibly using more flexible or low-friction cable materials. Additionally, fine-tuning the cable tension is recommended to align with ergonomic standards and enhance user control during shifting [18].

Furthermore, it was noted that the manufacturing tolerances of the bushing and bearing housings affected the rotational efficiency of the shafts. In some cases, the fit between the bushing and bearing was either too tight or too loose, which caused either excessive drag or vibration. As a solution, tighter quality control should be implemented during fabrication, especially in turning and milling processes, to ensure consistent tolerances and better alignment of rotating components.

4. Conclusion

This research successfully carried out the design, fabrication, and performance evaluation of a customized transmission system for the Garuda UNY UG-24 urban vehicle. Through the implementation of the 4D development method (Define, Design, Develop, and Disseminate), the transmission was adapted to meet the vehicle's high-torque demands. The performance test demonstrated a 75% success rate in gear shifting smoothness and overall functionality, although several technical weaknesses were identified. These findings provide valuable insights for future improvements and establish a solid foundation for further optimizing energy-efficient vehicle systems.

Conflict of interest

The authors declare no conflict of interest.

References

[1] G. P. Mustaqim and T. Wahjoedi, "Effectiveness of Student Participation in Campus Organizations," *INCOME: Innovation of Economics and Management,* vol. 3, no. 3, pp. 29-35, 2024.

[2] K. Haryana, Z. Arifin, I. N. Yoga, N. W. Purnomo, and M. Z. Naresworo, "The effect of tire pressure on car fuel consumption Garuda urban gasoline 19, in the Shell Eco-Marathon competition Asia 2019, Malaysia," 2024, vol. 3145: AIP Publishing, 1 ed., doi: https://doi.org/10.1063/5.0216922.

[3] T. Paul, "Design of chassis, impact attenuator, suspension and aerodynamic systems of a formula SAE car," 2019.

[4] D. C. Barton and J. D. Fieldhouse, *Automotive Chassis Engineering*. Springer, 2018.

[5] W. Zhang and J. Xu, "Advanced lightweight materials for Automobiles: A review," *Materials & Design,* vol. 221, p. 110994, 2022, doi: https://doi.org/10.1016/j.matdes.2022.110994.

[6] G. Lechner and H. Naunheimer, *Automotive transmissions: fundamentals, selection, design and application*. Springer Science & Business Media, 1999.

[7] M. R. Ahssan, M. Ektesabi, and S. Gorji, "Gear ratio optimization along with a novel gearshift scheduling strategy for a two-speed transmission system in electric vehicle," *Energies,* vol. 13, no. 19, p. 5073, 2020, doi: https://doi.org/10.3390/en13195073.

[8] S. Zhou, J. Liu, C. Li, and B. Wen, "Nonlinear behavior of a spur gear pair transmission system with backlash," *Journal of Vibroengineering,* vol. 16, no. 8, pp. 3850-3861, 2014.

[9] X. Li, Q. Cao, X. Zhang, and X. Gao, "Research on the influence of backlash and bearing clearance on torsional vibration of pure electric vehicle gear system," *International Journal of Vehicle Noise and Vibration,* vol. 17, no. 3-4, pp. 273-288, 2021, doi: https://doi.org/10.1504/IJVNV.2021.123435.

[10] R. B. Indaryanti, H. Harsono, S. Sutama, B. Murtiyasa, and B. Soemardjoko, "4D Research and Development Model: Trends, Challenges, and Opportunities Review," *Jurnal Kajian Ilmiah,* vol. 25, no. 1, pp. 91-98, 2025, doi: https://doi.org/10.31599/na7deq07.

[11] M. V. Zernin, A. V. Mishin, N. N. Rybkin, S. V. Shil'Ko, and T. V. Ryabchenko, "Consideration of the multizone hydrodynamic friction, the misalignment of axes, and the contact compliance of a shaft and a bush of sliding bearings," *Journal of Friction and Wear,* vol. 38, pp. 242-251, 2017, doi: https://doi.org/10.3103/S1068366617030163.

[12] J. Singh, A. Verma, R. Kunal, A. Balpande, and M. Dhane, "Shifter fork stiffness correlation to gear shift quality," *SAE International Journal of Commercial Vehicles,* vol. 6, no. 2013-01-2447, pp. 498-509, 2013, doi: https://doi.org/10.4271/2013-01-2447.

[13] W. Luo, G. Liu, and H. Wang, "Study on Anti-backlash Mechanism Used in Precise Transmission: A Review," 2021: Springer, pp. 1449-1470, doi: https://doi.org/10.1007/978-981-16-7381-8_89.

[14] W. Tang, Y. Zhou, H. Zhu, and H. Yang, "The effect of surface texturing on reducing the friction and wear of steel under lubricated sliding contact," *Applied surface science,* vol. 273, pp. 199-204, 2013, doi: https://doi.org/10.1016/j.apsusc.2013.02.013.

[15] D. T. Jelaska, *Gears and gear drives*. John Wiley & Sons, 2012.

[16] H. Du, W. Xiong, H. Wang, and Z. Wang, "A review: virtual assembly of flexible cables based on physical modeling," *Assembly Automation,* vol. 40, no. 2, pp. 293-304, 2020, doi: https://doi.org/10.1108/AA-04-2018-056.

[17] M. Blomgren, "Modeling and control of engaging gears in gearboxes without synchromesh towards specific angles between gear and coupling sleeve," ed, 2019.

[18] E. Garosi, F. Sheikh, and M. Goodarzi, "Ergonomic Interventions in Risk Reduction," 2025, doi: 10.5772/intechopen.1008463.